Enhancement of electrically small antennas properties with metamaterials

Master Thesis Project

Mobile Communication/
P10 project, spring semester 2010
Faculty of engineering, health care and natural sciences
Institute for Electronic Systems

Samantha CAPORAL DEL BARRIO

May, 31 2010

AALBORG UNIVERSITET

Aalborg University
Departement of Electronic Systems
Frederik Bajers Vej 7
9220 Aalborg O
Telephone 99 40 86 00
http://es.aau.dk

Title: Enhancement of electrically small antennas properties with metamaterials

Semester Theme : Master Thesis

Project term : P10, spring semester 2010

Author: Samantha CAPORAL DEL BARRIO

Supervisors : Ivan Bonev Bonev and Gert F. Pedersen

Number of copies : 4

Number of pages: 92

Completed : June 2010

Synopsis:

The purpose of this project was to understand the use of metamaterials in electrically small antennas and to enhance their properties with them.
For this purpose different kinds of metamaterials have been studied and discussed. The S-shaped metamaterial has been transform and adapted to the mobile phone requirements to obtain a small Z antenna. Different possible structures have been simulated in order to get the biggest enhancement for the resulting antenna.
The Z antenna for mobile phones application is naturally matched to the source, without the need of an additional circuit. Also, it enhances the gain, reduces the reactive near fields and is more resistant to the user's body influence.
Two papers have been submitted to present these results.

Preface

This report is separated into these three items :

Item 1: The main report on the analysis, simulation and explanation of a proposed antenna structure that includes metamaterials.

Item 2: Appendices in the end of the report

Item 3: Submitted papers for publication

Reading directions

Sources are given by [number], e.g. [10], referring to an index number in the sources list.

Samantha CAPORAL

Abbreviations

SRR	Split Ring Resonator
HPBW	Half-power bandwidth
PCB	Printed Circuit Board
SAR	Specific Absorption rate
AP	Accepted power
SWR	Standard wave ratio
PEC	Perfect electric conductor
FDTD	Finite-difference time domain
ENG	Epsilon negative
MNG	Mu negative
DNG	Double negative

Chapter 1

INTRODUCTION

The proliferation of wireless devices for communication has restimulated interest in efficient, broad-bandwidth, electrically small antennas. Antennas that are electrically small, are efficient, have significant bandwidth, are inexpensive and easy to build, and integrate simply into more complex systems would fill the needs of many new generation wireless systems [1].

Unfortunately, these requirements are contradictory when traditional electrically small antennas designs are considered ; compromises have to be done. The use of new artificial materials called metamaterials can help to improve the performances of the electrically small antennas, because they allow for unconventional electromagnetic properties that are not readily available in nature to be exploited.

1.1 Traditional electrically small antennas designs

The dimensions of handsets antennas are very small compared with the operating wavelength, particularly in the low bands. Not only is the antenna small, but the wavelength of the handset to which it is attached –typically between 80 and 100mm- is also only a fraction of a wavelength long [2].

For instance, at 915MHz the wavelength is : λ=0.41m.

Note that at these low frequencies, it is the whole phone that resonates [3].

A simple small antenna is shown in Fig. 1.1 where a short monopole is fed against a groundplane.

These antennas in Fig. 1.1 look capacitive at low frequencies, the input impedance has the form : Zin=R+jX, where R is small and X is very large [2].

The volume occupied by the antenna is highly related to the Q-factor, which relates the stored energy and the dissipated energy [2]. The bandwidth will be limited by the Q-factor of the device, where Q=X/R.

An electrically small antenna has a very reactive input impedance with an associated very narrow bandwidth [2].

Also, the radiation resistance of the small antenna is very small so it must carry a large current to radiate any significant power. Unfortunately the radi-

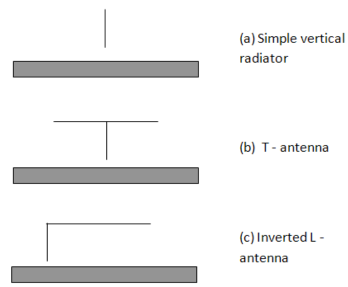

Figure 1.1: Short radiators over ground

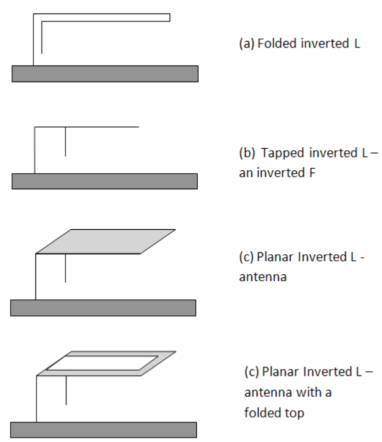

Figure 1.2: Derivatives of an inverted-L antenna

ation resistance may be comparable with the loss resistance in its conductors. Any current will create losses as well as radiation, therefore there is a problem with efficiency. Generally, a matching circuit is added to these antennas.

In the first case of Fig. 1.1 (a), the current at the top of the vertical radiator is zero and it rises linearly to some maximum value at the bottom[ref]. By extending a horizontal conductor from the top of the antenna, as shown in (b) and (c) the zero-current is moved to the end of the horizontal section and a larger and almost constant current flows now in the vertical section. The radiation resistance has been increased and the capacitive reactance reduced at the feedpoint. Consequently, the Q of the antenna has fallen.

This last design of electrically small antenna 1.1 (c) is known as Inverted-L antenna.

Further, other designs have been proposed Fig. 1.2

All these designs increase the value of the radiation resistance. The strongest resonance will be achieved when the upper limb will reach $\lambda/4$ and the position of the feedpoint will allow the impedance to be close to 50 ohms.

1.2 Metamaterials

1.2.1 Definition

"In general, metamaterials are artificial, man-made structures not found in nature. They gain their properties from their overall structure rather than directly from their composition and may have unusual properties also not found in nature." MITRE's Steven Best

It is the physicist VESELAGO who firstly imagined in 1967 such an artificial material and the possible wave propagation through it [4], with the vector triplet ($\mathbf{E}$,$\mathbf{H}$,$\mathbf{k}$) being indirect and giving the qualification of left-handed material.

They consist of arrays of structures in which both the individual elements and the unit cell are small compared to the wavelength of operation. When they are described by the conventional electromagnetic constants of permittivity and permeability, they show values that could not previously be obtained.

1.2.2 Metamaterials in small antennas

The main innovation is the introduction of a parasitic element in the very reactive near field of the electrically small radiator.

Adding this element in the mobile phones, it is expected :

- a reduction in the size of the antenna
- an improvement in the matching to the source
- a reduction in the near fields
- a reduction of the peak Specific Absorbtion Rate (SAR)
- to be more efficient with respect to the interaction with the user (head and hand)
- an enhancement in the gain
- a reduction in the coupling between two close antennas

Let's first remind the essential parameters for describing an antenna.

Chapter 2

THEORETICAL BACKGROUND

2.1 BASIC ANTENNA THEORY

To understand how antennas re-radiate energy and build them in the most efficient way, the following parameters are essentials to be presented. The performance of an antenna can be evaluated through them.

2.1.1 Field regions

The space surrounding an antenna is usually subdivided into three regions:

- the reactive near-field,
- the radiating near-field (Fresnel zone)
- the far-field (Fraunhofer zone) [5]

The Reactive near-field region is the portion of the near-field region immediately surrounding the antenna wherein the reactive field predominates. For most antennas, the outer boundary of this region is commonly taken to exist at a distance from the antenna surface, where λ is the wavelength and D is the largest dimension of the antenna.[5]

The Radiating near-field (Fresnel) region is the region of the field of an antenna between the reactive near-field region and the far-field region wherein radiation fields predominate and wherein the angular field distribution is dependent upon the distance from the antenna.[5]

The Far-field (Fraunhofer) region is the region of the field of an antenna where the angular field distribution is essentially independent of the distance from the antenna. If the antenna has a maximum overall dimension D, the far-field region is commonly taken to exist at distances greater than $R < \frac{2D^2}{\lambda}$ from the antenna, λ being the wavelength.

The figure 2.1 shows these different regions.

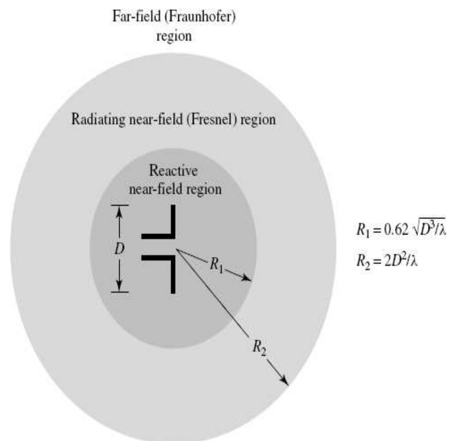

Figure 2.1: Field regions of an antenna

2.1.2 Radiation power density

Power and energy are associated with electromagnetic fields. In order to describe the power with association with an electromagnetic wave it is necessary to be used the Poynting vector. The Poynting vector is defined as [5] :

$$\overrightarrow{W} = E * H \tag{2.1}$$

where :
W is the instantaneous Poynting vector (W/m^2)
E is the instantaneous electric-field intensity (V/m)
H is the magnetic field intensity (A/m)
The total power which crosses a closed surface can be obtained by integrating the Poynting vector over the entire surface [5] :

$$P = \oint \overrightarrow{W}.d\overrightarrow{S} \tag{2.2}$$

where P is the instantaneous total power (expressed in Watt).
Furthermore, the average power density (time average Poynting Vector) can be calculated using the following equation [5]:

$$W_{av} = \frac{1}{2}Re(\overrightarrow{E}.\overrightarrow{H}) \tag{2.3}$$

Therefore, the average power radiated by an antenna can be written as [5]:

$$P_{rad} = P_{av=} \oint \overrightarrow{W_{rad}}.d\overrightarrow{S} = \frac{1}{2}\oint Re(\overrightarrow{E}.\overrightarrow{H}).d\overrightarrow{S} \tag{2.4}$$

2.1.3 Radiation intensity

The radiation intensity is defined as the power radiated from an antenna per unit solid angle. The formula to calculate it is [5]:

$$U = r^2 * W_{rad} \tag{2.5}$$

where :
U is the radiation intensity (W/unit solid angle)
W_{rad} is the radiation intensity (W/m^2)

2.1.4 Directivity

The directivity of an antenna is defined as the ration between its radiation intensity in a given direction and that of an isotropic source. The directivity of an antenna is expressed as following [5]:

$$D = \frac{U}{U_0} = \frac{4\pi U}{P_{rad}} \tag{2.6}$$

If the direction is not specified, the expression for the maximum directivity (the direction of maximum radiation intensity) is :

$$D_{max} = D_0 = \frac{U_{max}}{U_0} = \frac{4\pi U_{max}}{P_{rad}} \tag{2.7}$$

where :
D is the directivity (dimensionless)
D_0 is the maximum directivity (dimensionless)
U is the radiation intensity (W/unit solid angle)
Umax is the maximum radiation intensity (W/unit solid angle)
U_0 is the radiation intensity of isotropic source (W/unit solid angle)
P_{rad} is the total radiated power (W)

2.1.5 Accepted power

The Accepted Power (AP) is the power delivered to the antenna terminals from the source. It contains information about any mismatch between the source, the feedline, and the antenna. The AP can be expressed in function of the reflection coefficient and the input power (P_{in}). Let's consider the transmission line in Fig.2.2 between a source and an antenna :

P_{in} is the input power of the source,

Z_0 is the characteristic impedance of both the source and the feedline (assuming here that the feedline is matched to the source),

Z_{in} is the input impedance of the antenna.

The reflection coefficient at the antenna is [1]:

$$\Gamma = \frac{Z_{in} - Z_0}{Z_{in} + Z_0} \tag{2.8}$$

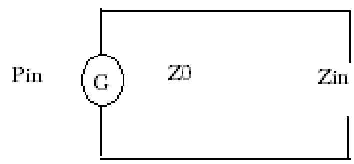

Figure 2.2: Transmission line between the source and the antenna

The AP by the antenna is then [1]:

$$AP = (1 - |\Gamma|^2)P_{in} \tag{2.9}$$

2.1.6 Mismatch loss

The corresponding mismatch to the accepted power is : $\frac{AP}{P_{in}} = 1 - |\Gamma|^2$. This quantity is also called : Accepted Power efficiency (AE).

The mismatch loss is generally expressed in absolute value, in dB :

$$ML(dB) = -10log(1 - \Gamma^2) = -10log(1 - (10^{\frac{-s_{ii}}{20}})^2) \tag{2.10}$$

2.1.7 Antenna efficiency

Several efficiencies are used to characterize small antennas, mainly the radiation efficiency e_r and the total efficiency e_t. Both are presented in this section.

The radiation efficiency corresponds to the amount of power that propagates into the far-field from the power delivered to the terminals of the antenna.

The radiation efficiency can be seen as [1]:

$$e_{rad} = \frac{P_{rad}}{AP} = AP - \text{power dissipated in the antenna} \tag{2.11}$$

The overall efficiency e_t takes into account all of the possible losses. It is used to evaluate the losses at the input terminal and within the structure of an antenna. This losses may due to :

- reflections
- conduction and dielectric losses

The overall efficiency e_t can be written as [5]:

$$e_t = e_r e_c e_d \tag{2.12}$$

where :
e_t is the total efficiency (dimensionless)

e_r is the reflection efficiency, it is equal to 1-$|s_{11}|^2$ (dimensionless)

where : s_{11} is the voltage reflection coefficient at the input terminal of the antenna [section 2.3]

e_c is the conduction efficiency (dimensionless)

e_d is the dielectric efficiency (dimensionless)

It is quite difficult to compute e_c and e_d, but they can be determined experimentally using the connection $e_{cd} = e_c * e_d$. e_{cd} is called the antenna radiation efficiency, it is related to the gain and the directivity.

The effect of the user and the phone box have to be included for the absorption. By using FDTD, this analysis can be performed. Indeed, it has been found that between 50% and 70% of the power may be absorbed, depending on the distance from the antenna to the surface of the user's head. [5]

Another way to express the overall efficiency is :

$$e_t = \frac{P_{rad}}{P_{in}} \tag{2.13}$$

corresponding to the portion of the input power that is radiated into the far-field of the antenna.[1]

2.1.8 Gain

The gain of an antenna is related to the directivity. It is defined as the ratio between the intensity in a given direction ant the radiation intensity that would be obtained if the power accepted by the antenna would be radiated isotropically. For an isotropically radiated power radiation intensity, it is equal to the power accepted by the antenna divided by 4π. The corresponding formula is:

$$Gain = 4\pi \frac{radiation\ intensity}{total\ input\ power} = 4\pi \frac{U(\vartheta, \varphi)}{P_{in}} \tag{2.14}$$

Losses from polarization and impedance mismatch are not included in this gain, but the absolute gain takes into account all reflection/mismatch losses. Furthermore, these two gains can be equal when the antenna input impedance Zin is equal to the characteristic impedance Zc of the line, in other words when the antenna is perfectly matched to the transmission line.

The gain can be related to the overall efficiency and the directivity as follows:

$$Gain = e_t * D \tag{2.15}$$

2.1.9 Conclusion

All these parameters are usefull to evaluate the performance of an antenna. Some of them are related. It is by the analysis and the combination of all of them that the performance of an antenna can be evaluated.

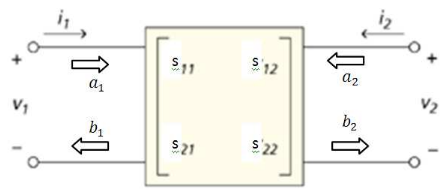

Figure 2.3: Incoming and outgoing waves for a two-port network

2.2 S-PARAMETERS

2.2.1 Mathematical calculation

To characterize microwave networks, the scattering (or S-) parameters must be employed. The S-parameters are defined in terms of wave variables, which are more easily measured at high frequencies than voltage or current, used in more basic methods for circuit analysis.[6]

The S-parameters are fixed properties of the linear circuit. They are useful for describing how the energy couples between two ports connected to a circuit, as illustrated in Fig. 2.3.

A two ports network as shown above -with one input and one output- can be described by the following equations :

$$b_1 = s_{11}a_1 + s_{12}a_2 \tag{2.16}$$

$$b_2 = s_{21}a_1 + s_{22}a_2 \tag{2.17}$$

[6]

where a_1 and a_2 are the incident voltage wave variables, while b_1 and b_2 are the scattered voltage waves. These two equations lead to the matrix of the two port network :

$$b = S\,a \tag{2.18}$$

where $b = \begin{pmatrix} b_1 \\ b_2 \end{pmatrix}$, $S = \begin{pmatrix} s_{11} & s_{12} \\ s_{21} & s_{22} \end{pmatrix}$ and $a = (a_1 a_2)$.

The S-parameters are calculated assuming that one incident voltage is equal to zero, as follows [6] :

$$s_{11} = (\frac{b_1}{a_2})|_{a_2=0}$$

$$s_{21} = (\frac{b_2}{a_1})|_{a_1=0}$$

$$s_{12} = (\frac{b_1}{a_2})|_{a_1=0}$$

$$s_{22} = (\frac{b_2}{a_2})|_{a_1=0} \tag{2.19}$$

Therefore, the S-parameters are dimensionless. The S-parameters can also be expressed in decibels applying the following formula [6] :

$$s_{ij}(dB) = 20log_{10}|s_{ij}| \tag{2.20}$$

The relationship between S-parameters, total voltage and total current can be obtained with the reference impedance at each port [6].

For port k :

$$\begin{pmatrix} a_k \\ b_k \end{pmatrix} = \begin{pmatrix} 1 & Z_{0k} \\ 1 & -Z_{0k} \end{pmatrix} \begin{pmatrix} V_k \\ I_k \end{pmatrix} \quad , \; k = 1, 2 \tag{2.21}$$

Therefore, the S-parameters can be calculated with impedances only, using the reference impedances and defining the input impedances at each port $Z_{in1}$and Z_{in2} [6] :

$$s_{11} = (\frac{b_1}{a_2})|_{a_2=0} = \frac{V_1 - Z_{01}I_1}{V_1 + Z_{01}I_1} = \frac{Z_{in1} - Z_{01}}{Z_{in1} + Z_{01}} \tag{2.22}$$

The other terms of the S-matrix can be calculated in a similar way.

2.2.2 Physical meaning

The S-matrix can be extended to a n-port network. Each term of the S-matrix has a physical meaning.

2.2.2.1 The return loss

The diagonal terms, s_{ii}, are called return loss terms. In a two ports network, $s_{11}$is the input return loss and s_{22} is the output return loss, they give a measure of the scattered energy caused by impedance mismatches in the system, i.e. the ration of the reflected power to the incident power [6]. The same definition can be applied to a n port network, when all ports are matched.

$$s_{ii}(dB) = 10log_{10}\left(\frac{P^+}{P^-}\right) \tag{2.23}$$

Since $P^- = |\Gamma_n|^2 P^+$, Γ_n being the reflection coefficient at port n, the return loss can also be defined as :

$$s_{ii}(dB) = -20log_{10}\left(|\Gamma_n|\right) \tag{2.24}$$

Therefore, the larger the return loss , the smaller the reflection coefficient. The minimum acceptable value for the return loss is 20dB [6]. Any larger value will mean less reflection, so better transmission.

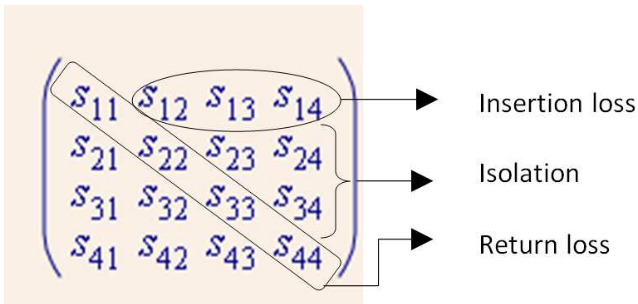

Figure 2.4: Interpretation of each element of the S-matrix

2.2.2.2 The insertion loss

For one fixed port, the insertion loss is the reduction of signal strength during transmission to the other. For instance, s_{12} is from port 1 to port 2. This definition can be extended to n-port system:

$$s_{ij}, \quad 2<j<n$$

is the loss in the transmission from port 1 to port j. As it is a loss, the value will be negative in dB.

2.2.2.3 The isolation

The isolation is a measure of the voltage or power gain from output port i to output port j [6].

$$s_{ij}, \quad i\ddagger j$$

When the gain is zero, there is perfect isolation. Generally, -20 dB isolation is required in industry [6]. In the following 44-matrix, the definition of S-parameters are summarized : Fig. 2.4

2.2.3 Conclusion

The S-parameters are a way to describe the electrical behavior of the input signal much more adapted to multiport microwave networks.

In mobile phone applications, the s_{11} and s_{21} parameters are the mostly used S-parameters. The s_{11} gives a measure of the matching of an antenna, the actual requirements consider that anything greater than 20dB is acceptable. The s_{21}gives a measure of the coupling between two close antennas. Wen they are both receiving or both transmitting, tey shoul not interfer with each other and be totally isolated. Therefore, the best value expected for s_{21}would be zero, regarding antenna 1.

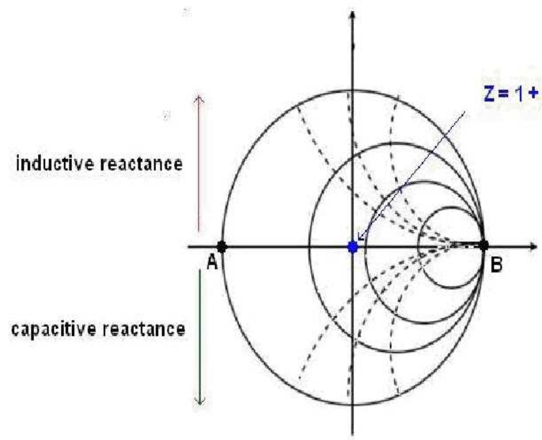

Figure 2.5: Smith Chart with important areas

2.3 SMITH CHART

The Smith Chart is widely used and permits to solve and understand transmission line problems graphically. It allows to represent the impedance variation of a dipole in terms of frequency, to calculate the load impedance seen through a line and to size a matching circuit impedance. The impedance, Z = R ± jX can be plotted on the Smith Chart.

2.3.1 Description

At the first glance, it is possible to distinguish some benchmarks.

Point A is the origin of the abscissa axis, where the resistance is equal to zero (Fig. 2.5). Point B is the end of the abscissa axis, where the resistance and the reactance are infinity. On the axis AB, the reactances are zero and therefore, there are only pure resistances. The upper half of the graph is the area of inductive reactance and the lower one is the area of capacitive reactance [7].

2.3.2 Impedance plotting

The impedance can be plotted in terms of its two components R and X. The values of the reactances and resistances are defined by circles and lines as it is shown on Fig. 2.6

All points on the same circle represent the same resistive component, and all points on the same line - the same reactance. Those above the abscissa axis are capacitive reactances and those below are inductive reactances. The impedance in terms of Z = R ± jX can be plotted on the Smith Chart as it is shown on Fig. 2.7

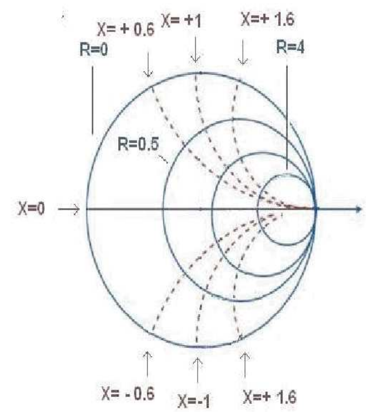

Figure 2.6: Lines and circles description of the Smith Chart

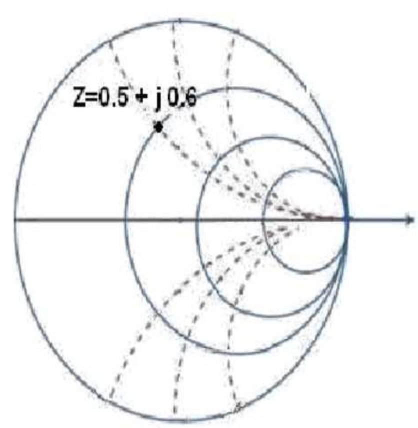

Figure 2.7: Impedance plotted on a Smith Chart

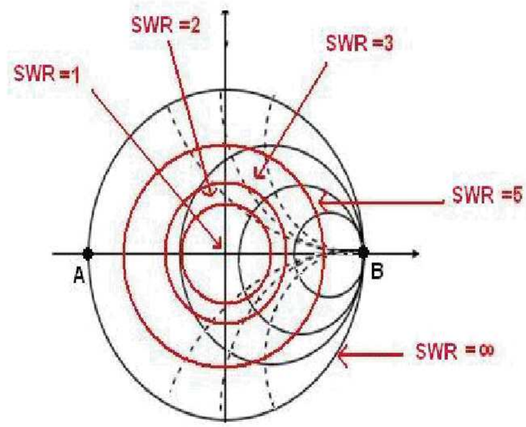

Figure 2.8: Circles of SWR on the Smith Chart

The impedance is at the intersection point of the resistance circle with the line of the reactance as it can be seen on Fig. 2.7 [7].

2.3.3 SWR and loss

Another type of circles which are not plotted on the graph are the Standing-Wave- Ratio or SWR circles. They are concentric circles (Fig. 2.8) and all points on the same SWR circle have the same SWR and reciprocally two different impedances with the same SWR are plotted on the same SWR circle.

The SWR circle is easy to be traced because the radius corresponds to the distance between the central point Z = 1 + j0 and the plotted impedance.

If the line is lossless, the SWR is constant whatever the place of the measurement is. If the line have losses, then the amplitude of the reflected wave decreases as the distance from the charge gets bigger (Fig. 2.9). In this case part of the energy is dissipated due to the losses in the line.

In the same way, the amplitude of the incident wave increases as the distance from the generator increases. The reflection coefficient and the SWR are bigger nearer to the load than closer to the generator [7].

2.3.4 Formulas

The SWR, the reflection coefficient and the return loss are related as following:

$$\Gamma = \frac{SWR-1}{SWR+1}\,, \quad SWR = \frac{1+\Gamma}{1-\Gamma}$$

$$RL = s_{ii}(dB) = -20log(\Gamma)\,, \quad SWR = \frac{1+10^{\frac{-RL}{20}}}{1-10^{\frac{-RL}{20}}}$$

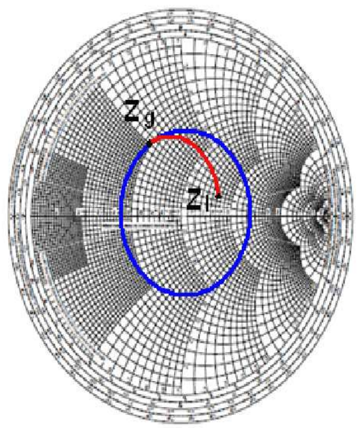

Figure 2.9: Influence of losses on the SWR

2.4 PERMITTIVITY-PERMEABILITY

Because every material is a composite, even if the individual ingredients consist of atoms and molecules, it has been defined the permittivity ε and the permeability μ of a material to present an homogeneous view of the electromagnetic properties [8].

Let's remember that :

$$D = \varepsilon E \quad and \quad B = \mu H \tag{2.25}$$

where :
D is the electric displacement (C/m^2)
$\varepsilon = \varepsilon_0 \varepsilon_r$ (F/m) , $\varepsilon_0 = 8.85 * 10^{-12} F/m$ is the permittivity of free space
E is the electric field (V/m)
B is the magnetic field (W/m^2)
$\mu = \mu_0 \mu_r$ (H/m), $\mu_0 = 4\pi * 10^{-7} H/m$ is the permeability of free space
H is the modification of B due to magnetic fields produced by the material media (A/m)

The permittivity is a measure of how much a medium changes to absorb electrical energy when subjected to n electrical field.

The permeability is a constant of proportionality that exists between magnetic induction and magnetic field Intensity.

Both ε and μ can take real or complex values.

$$\varepsilon(\omega) = \varepsilon'(\omega) + j\varepsilon''(\omega) \quad and \quad \mu(\omega) = \mu'(\omega) + j\mu''(\omega) \tag{2.26}$$

ε' is the real part of the permittivity, which is related to the stored energy within the medium.

ε" is the imaginary part of the permittivity, which is related to the dissipation (or loss) of energy within the medium : $\sigma(\omega) = \omega\varepsilon''(\omega)$

For the permittivity, the ratio of the imaginary to the real part of the complex permeability is called the loss tangent. It provides a measure of how much power is lost in a material versus how much is stored [9][10].

Chapter 3

METAMATERIALS

A classification of the different materials can be done as shown in Fig. 3.1.

This common classification is divided in four parts corresponding to all of the composition of the signs of the permeability and permittivity of a material [11].

Double positive media (DPS) do occur in nature such as naturally occurring dielectrics. Permittivity and magnetic permeability are both positive and wave propagation is in the forward direction.

Epsilon negative media (ENG) – permittivity ε is negative while permeability µ is positive. Many plasmas exhibit this characteristic. For example noble metals such as gold or silver will exhibit this characteristic in the infrared and visible spectrums.

Mu-negative media (MNG) – permeability µ is negative while permittivity ε is positive.

In the two last media, ENG and MNG, the waves are not allowed to propagate into uniform medium. As the wave propagation in isotropic homogeneous media is function of $e^{\pm jkx}$where the wave number is $k = \sqrt{\mu\varepsilon}$, the square roots gives an imaginary wave number.

Double negative media (DNG) have both permittivity and permeability are negative resulting in a negative index of refraction.The materials with these properties are called metamaterials. The following section will focus on this particular case.

3.1 Definition of metamaterials

A metamaterial is an artificially composite structure having interesting effective properties, especially at wavelengths much greater than the unit size [8].

Particular phenomena were observed in such materials like the inversion of the inversion of the Doppler effect or the law of Snell-Descartes, from here comes the appellation left-handed media.

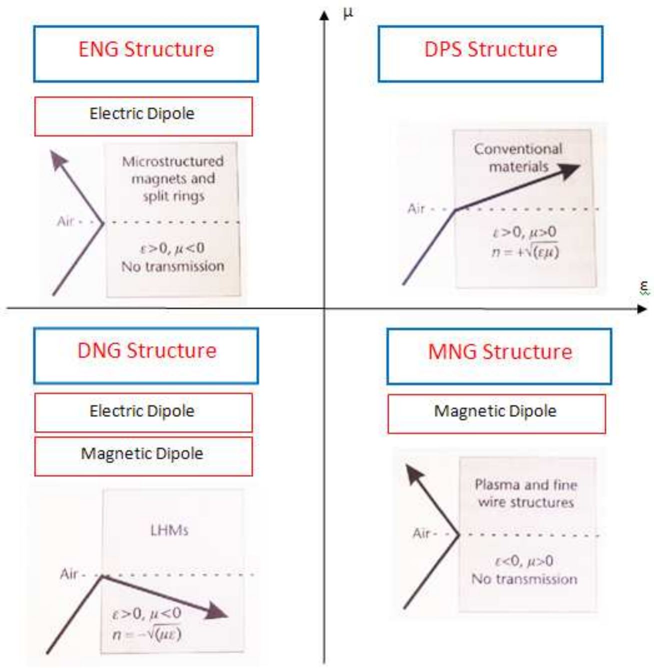

Figure 3.1: Basic classification of materials regarding permittivity and permeability signs

Other terms that have been proposed for media with simultaneously negative ε and μ are negative-refractive media, backward media, double negative media and also Veselago media.

3.2 The electrodynamics of left handed media

3.2.1 Propagation allowed

The propagation constant of a plane wave is given by $k = \omega\sqrt{\varepsilon\mu}$, so it is apparent that the wave propagation is not forbidden in left-handed media.

3.2.2 Wave propagation in left-handed media

From the Maxwell's equations, it can be shown that the wave equation is [11]:

$$\left(\frac{\nabla^2 - \frac{n^2}{c^2}\partial^2}{\partial t}\right)\varphi = 0 \tag{3.1}$$

where :
n is the refractive index,

c is the velocity in the vacuum, $n^2/c^2 = \varepsilon\mu$.

The squared refractive index is unchanged by simultaneous change of permittivity and permeability, meaning that the left-handed media is transparent [11].

However, the solutions of the wave equation are quite different for this media. Let's consider the plane wave fields $\overrightarrow{E} = \overrightarrow{E_0}e^{(-j\overrightarrow{k}.\overrightarrow{r}+j\omega t)}$ and $\overrightarrow{H} = \overrightarrow{H_0}e^{(-j\overrightarrow{k}.\overrightarrow{r}+j\omega t)}$. The curl equations :

$$\nabla \times \overrightarrow{E} = -j\omega\mu\overrightarrow{H} \tag{3.2}$$

$$\nabla \times \overrightarrow{H} = j\omega\varepsilon\overrightarrow{E} \tag{3.3}$$

Can be reduced to :

$$\overrightarrow{k} \times \overrightarrow{E} = \omega\mu\overrightarrow{H} \tag{3.4}$$

$$\overrightarrow{k} \times \overrightarrow{H} = -\omega\varepsilon\overrightarrow{E} \tag{3.5}$$

Therefore, for positive ε and μ, $\overrightarrow{E}$,$\overrightarrow{H}$ and $\overrightarrow{k}$ form a right-handed orthogonal system of vectors.

But, if ε and μ are negative, the above equations can be rewritten as :

$$\overrightarrow{k} \times \overrightarrow{E} = -\omega|\mu|\overrightarrow{H} \tag{3.6}$$

$$\overrightarrow{k} \times \overrightarrow{H} = \omega|\varepsilon|\overrightarrow{E} \tag{3.7}$$

and it becomes apparent that $\overrightarrow{E}$,$\overrightarrow{H}$ and $\overrightarrow{k}$ now form a left-handed triplet as illustrated in the Fig. 3.2.

Also, the direction of the energy is determined by the real part of the Poynting vector :

$$\overrightarrow{S} = \frac{1}{2}\overrightarrow{E}.\overrightarrow{H}* \tag{3.8}$$

which is unaffected by the simultaneous change of ε and μ.

Thus $\overrightarrow{E}$,$\overrightarrow{H}$ and $\overrightarrow{S}$ still form a right handed triplet in left-handed media. Therefore, in such media, energy and wavefronts travel in opposite directions.

This is shown in Fig. 3.2.

3.2.3 Energy density

3.2.3.1 Physical definition

If negatives ε and μ are introduced in the usual expression for the time-averaged density of energy given by :

$$U = \frac{1}{4}(\varepsilon|E|^2 + \mu|H|^2) \tag{3.9}$$

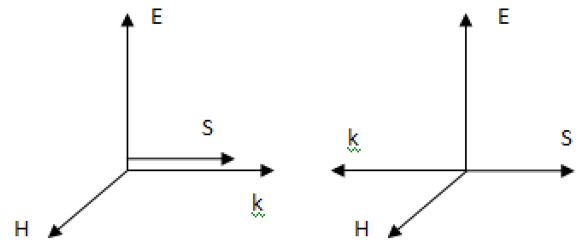

Figure 3.2: Illustration of the system of vectors E, H, k and S for a plane transverse electromagnetic (TEM) wave in an ordinary (left figure) and left-handed (right figure) media

They produce the non physical result of a negative density of energy.

3.2.3.2 Considering a dispersive medium

But, using the correct expression for a quasimonochromatic wavepacket [11] traveling in a dispersive medium :

$$U = \frac{1}{4}(\frac{\partial(\omega\varepsilon)}{\omega}|E|^2 + \frac{\partial(\omega\mu)}{\omega}|H|^2) \tag{3.10}$$

So, for positive energy density, is the two partial derivatives that have to be positive :

$$\frac{\partial(\omega\varepsilon)}{\omega} > 0 \quad and \quad \frac{\partial(\omega\mu)}{\omega} > 0 \tag{3.11}$$

which is compatible with : $\varepsilon < 0$ and $\mu < 0$.

3.2.4 Group and phase velocities

Knowing that $k^2 = \omega^2\mu\varepsilon$, it comes that :

$$\frac{\partial k^2}{\partial\omega} = 2k\frac{\partial k}{\partial\omega} \equiv 2\frac{\omega}{v_p v_g} \tag{3.12}$$

It can be shown that $\frac{\partial k^2}{\partial\omega} < 0$ [11], therefore $v_p v_g < 0$.

This means that the wavepackets and wavefronts travel in opposite directions, and can be considered an additional proof of backward-wave propagation in physical left-handed media.

3.2.5 Doppler Effect

When a moving receiver detects the radiation coming from a source at rest in a uniform medium, the detected frequency of the radiation depends on the relative velocity of the emitter ant the receiver.[11] This is the well-known Doppler effect.

A straightforward calculation [11] shows that the frequency shifts are given by :

$$\triangle\omega = \omega_0 \frac{nv}{c} \tag{3.13}$$

where :
$\omega_0$is the frequency of the radiation emitted by the source,
v is the velocity at which the receiver moves towards the source,
c is the velocity of the light in free space,
n is the refractive index of the medium.
$\triangle\omega$is the difference between the frequency detected at the receiver and the frequency of oscillation of the source.

For n $<$ 0, the frequency shift becomes negative for positive v(receiver moving towards to the source). This means that the wave propagation is backwards and the wavefront moves towards the source. Thus, both receiver and wavefront move in the same direction and the frequency measured at the receiver is smaller than the frequency measured by an observer at rest.

3.2.6 Waves at interfaces

With the electromagnetic waves analysis, an interface between an ordinary and a left-handed medium will be considered.

A key magnitude in the analysis is the wave impedance of each medium, Z, which is defined as the ratio between the transverse component of the electric and magnetic fields.[11]

In Fig. 3.3, is shown how waves travel between two media of opposite sign.

The index i=1 (i=2) stands for the fields at the left-(right-)hand side of the interface, where $n_1 > 0$ and $n_2 < 0$. Positive waves are defined as those waves carrying enegy along the positive axis perpendicular to the interface. [11]

According to this wave definition, the impedance can be calculated as follow [11] :

$$Z_i = \frac{E^+_{y,\,i}}{H^+_{z,\,i}} = \frac{\omega\mu_i}{k_{x,\,i}} \tag{3.14}$$

In the left-handed medium, both µ and kx are negative, so the impedance is positive, as required for passive media. [11] The transmission, T, and reflection, R, coefficient are defined by[11] :

$$T = \frac{2Z_2}{Z_2 + Z_1}, \quad R = \frac{Z_2 - Z_1}{Z_2 + Z_1} \tag{3.15}$$

For the particular case of $Z_2 = Z_1$, it follows that T=1 and R=0. So, the left-handed media is perfectly matched to the ordinary one.

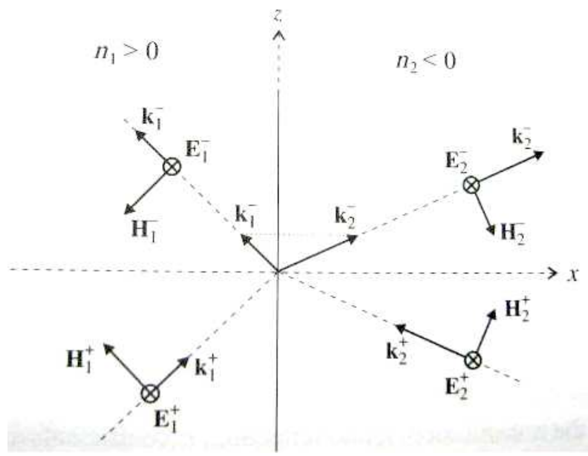

Figure 3.3: Definition of positive and negative waves at the interface between an ordinary medium and a left-handed medium. The Backward propagation in the left-handed medium has been taken into account in the definition of positive and negative waves.

3.3 Metamaterials construction

Left-handed metamaterials are artificial materials designed to have simultaneously negative values of permeability and permittivity over a finite frequency band. Such an artificial medium can be realized by using periodical arrays of split ring resonators (SRR) and thin wires together, as shown by the studies of Pendry and Smith [12].

The SRR array is used to obtain negative values of effective permeability while the thin wire array serves to produce negative values of effective permittivity.

The metamaterials gain their properties from their periodic structure (rather than composition) using the inclusion of small inhomogeneities for showing up a macroscopic behavior. [12]

3.3.1 Thin Wires

Nature provides us with a wide range of dielectric materials but one significant absence is materials with largely real and negative permittivity in the microwave regime.

For instance noble materials like gold or silver have a negative permittivity at very high frequencies but also an extremely large conductivity (or imaginary part of the permittivity).

The most popular material that can provide both real and negative permittivity is the thin wires structure. [10]

A very fine wire grid as shown in Fig. 3.4 leads to a permittivity equal to :

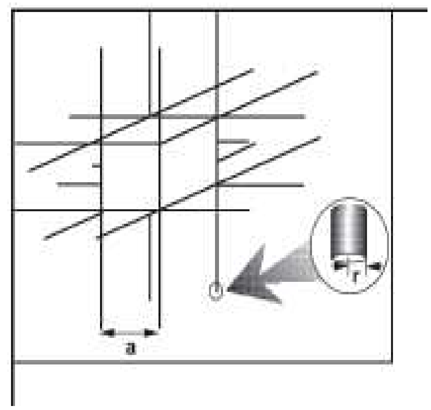

Figure 3.4: A fine wire structure

$$\varepsilon(\omega) = 1 - \frac{{\omega_p}^{\mathbf{2}}}{\omega(\omega + i\gamma)} \tag{3.16}$$

where : ${\omega_p}^{\mathbf{2}}$is the plasma frequency : ${\omega_p}^{\mathbf{2}} = \frac{2\pi c^2}{a^2 ln(\frac{a}{r})}$

How can be found this formula and the equivalence with the plasma deserve a more complete explanation.

3.3.1.1 Plasmas

Walter Rotmann studied the modeling of dilute plasmas – with plasma frequencies in the microwave regime – by systems of metallic wires. Many years later, Pendry addressed the same problem from a different standpoint. Because lossless plasmas exhibit a negative effective permittivity below plasma frequency, these works opened the way to the design of artificial media with negative dielectric permittivity.

3.3.1.2 ...from plasma to waveguide

In a rectangular metallic waveguide, the propagation constant is [11] :

$$k^{\mathbf{2}} = \omega^{\mathbf{2}} \varepsilon_0 \mu_0 (1 - \frac{{\omega_c}^{\mathbf{2}}}{\omega^{\mathbf{2}}}) \tag{3.17}$$

where $\omega_c$is the cutoff frequency of the waveguide. This dispersion is identical to that of an ideal plasma provided the cutoff frequency ω_c is substituted by the plasma frequency ω_p.

This identity suggest that a rectangular waveguide can be seen as one dimensional plasma with an effective dielectric constant of [11] :

$$\varepsilon_{eff} = \varepsilon_0 (1 - \frac{{\omega_c}^{\mathbf{2}}}{\omega^{\mathbf{2}}}) \tag{3.18}$$

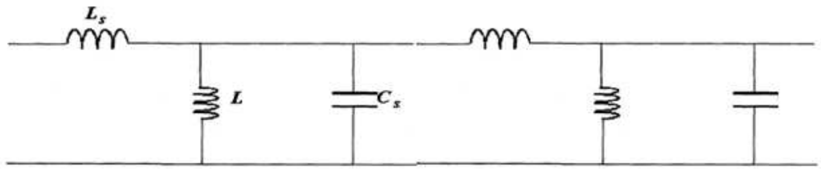

Figure 3.5: Illustration of the transmission line model for wire media

3.3.1.3 Equivalence thin wire array – plasma

Because continuous media relations are satisfied,

$$k^2 = \omega^2 \varepsilon_{eff} \mu_{eff} \quad and \quad Z^2 = \frac{\mu_{eff}}{\varepsilon_{eff}} \tag{3.19}$$

this equivalence plasma-waveguides can be extended to any hollow waveguide[11].

Therefore, a bunch of square waveguides will behave as a one-dimensional plasma.

The above result can also be extended to the simulation of a two-dimensional plasma by a system of parallel metallic plates such as those shown in Fig 3.4.

The propagation constant is the same that in the rectangular waveguide [11]. This media corresponds to an ideal plasma with plasma frequency $\omega_p = \omega_c = \frac{c\pi}{a}$, where a is the distance between the plates and c the speed of light.

3.3.1.4 Wire media

If the period of the wire mesh is smaller than the free space wavelength, the wire media should be approximately equivalent to the bunch of waveguides.[11]

The plasma frequency of such artificial plasma should be close to the cutoff frequency of the waveguide bunch : $\omega_p = \frac{c\pi}{a}$.

3.3.1.5 Equivalent transmission line

The equivalent transmission line for a wire medium is shown in Fig. 3.5:

Ls is the per unit length series inductance of the parallel plate transmission line. $\frac{L_s}{a} = \mu_0$,

C$_s$ is the per unit length shunt capacitance. $\frac{C_s}{a} = \varepsilon_0$.

3.3.2 Split Ring Resonators

The SRR array is used to obtain negative values of effective permeability.

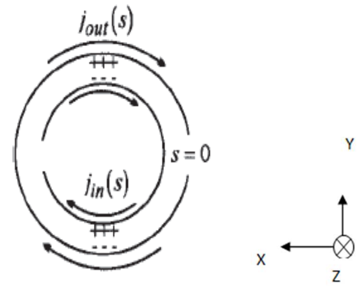

Figure 3.6: Induced currents in a SRR by a magnetic field

3.3.2.1 Geometry of a unit cell

In 1999, Pendry proposed an original metamaterial structure made of an array of metallic split-ring resonators. It consists in two concentric metallic split rings, printed on a microwave dielectric circuit board (Fig. 3.6). The important point is that there is a gap that prevents current from flowing around any one ring. However there is a considerable capacitance between the two rings, which enables current to flow. When it is excited by a time-varying external magnetic field directed along the z-axis, the cuts on each ring (placed on opposite sides) force the electric current to flow form one ring to another across the slots between them, taking the form of a strong displacement current. The slots between the rings therefore behave as a distributed capacitance. [11]

The greater the capacitance, the greater the current. [12]

3.3.2.2 Model

It has been shown [12] that SRRs behave as an LC resonator that can be excited by an external magnetic flux, with the self inductance being defined by the ring size and the capacitance by the gaps in and between the rings. Fig 3.7 shows the equivalent-circuit model for the SRR. In this figure, C0 stands for the capacitance between the rings. The resonance frequency of the SRR is given by $f_0 = \frac{1}{2\pi\sqrt{L_s C_s}}$, where Cs is the series capacitance of the upper and lower halves of the SRR, C_s=$C_0/4$. The inductance Ls can be approximated by that of a single ring with averaged radius r_a and width w.

The equation for the total current I on the circuit is given by :

$$\left(\frac{2}{j\omega C_s} + j\omega L_s\right) I = E \tag{3.20}$$

E being the external excitation.

The resonance frequency, ω_0, of the SRR can be obtained solving this equation for E=0 :

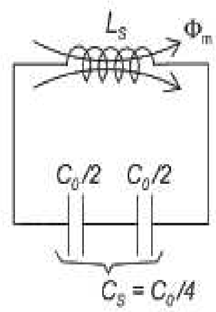

Figure 3.7: Equivalent circuit model of an SRR

$$\omega_0{}^{\mathbf{2}} = \frac{2}{L_s C_s} \tag{3.21}$$

Then, the equation for the total current when the SRR is exited by an external magnetic field : $-j\omega\phi_{ext}$becomes :

$$I = \frac{\phi_{ext}}{L_s}\left(\frac{\omega_0{}^{\mathbf{2}}}{\omega^{\mathbf{2}}} - 1\right)^{-1} \tag{3.22}$$

The SRR essentially behaves as a capacitively loaded conducting loop. It exhibits a resonant magnetic polarizability. [11]

3.3.3 Negative permeability

As mentioned before, the metamaterial get their unusual properties from the periodic structure, as shown in Fig. 3.8

Detailed calculations[11] give :

$$\mu_{eff(\omega)} = 1 - \frac{F}{1 + \frac{2\sigma i}{\omega r \mu_0} - \frac{3}{\pi^2 \mu_0 \omega^2 C r^2}} \tag{3.23}$$

where :
F is the fractional volume of one cell : $F = \frac{\pi r^2}{a^2}$
C is the capacitance between two rings : $C = \frac{\varepsilon_0}{d} = \frac{1}{dc^2\mu_0}$
σ is the resistance of the unit cell (per unit area)
d is the separation from one ring to the other for the same unit cell (m)
a is the separation between the ring centers (m)
r is the radius of one unit cell (m)
Then the effective magnetic permeability looks like in Fig. 3.9:

The Fig 3.9 shows a resonant structure dictated by the capacitance between the sheets and magnetic inductance of the cylinder. Below the resonant frequency, μ_{eff} is enhanced, but above resonance, μ_{eff} is less than unity and may be negatively close to the resonance. [12]

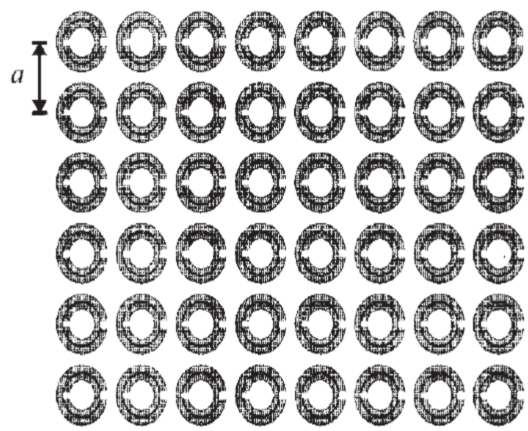

Figure 3.8: One layer of SRR

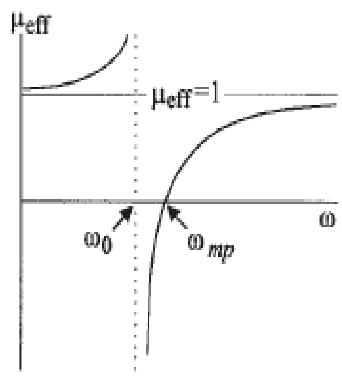

Figure 3.9: Effective permeability of a layer of SRRs

Pendry demonstrated [12] how to enhance nonlinear effects : most of electrostatic energy of the capacitor is located in the tiny gap between the rings . Then, concentrating most of the electromagnetic energy in this very small volume will results in an enormously enhanced energy density.

The strength of the metamaterial structure is to concentrate the electromagnetic energy in a very small volume, increasing its density by a huge factor, and greatly enhancing any nonlinear effects present.[12]

This structure is made from nonmagnetic thin sheets of metal, which respond to microwave radiation as if they had an effective magnetic permeability.[12]

A wide range of permeabilities can be achieved by varying the parameters of the structure.

3.3.4 Resonance behavior

In this section, will be presented the effects of substrate parameters on the resonant frequency.

- As the substrate thickness increases, the resonance frequency f_0 of the SRR unit cell decreases. This behavior is explained by the fact that the capacitance term Cs increases as the thickness gets larger. [13]

The resonance frequency is shifted lower as the two rings get closer. [13]

- The half-power bandwidth (HPBW) remains constant when the thickness changes and s shifted to lower values for closer rings.[13]
- As the thickness increases, the matching improves. [13]
- As the relative permittivity of the substrate increases, the resonant frequency decreases almost linearly [13]
- The HPBW decreases almost exponentially as the permittivity increases and the transmission minimum ($\min(|s_{11}|)$) increases almost exponentially.

3.4 Other SRR designs

The SRR originally proposed by Pendry may produce a strong magnetic polarizability near its resonance[11].

Because the SRR is electrically small at resonance, and it can be easily and reliably manufactured, its usefulness for the design of magnetic metamaterials is apparent.

However, some properties may be the origin of unwanted effects [11] and the capacitance between the rings does not increase so much by reducing the distance between the rings(with practical values). Therefore, the frequency of resonance cannot be made too small.

Such limitations can be overcome by modifications in the designs :

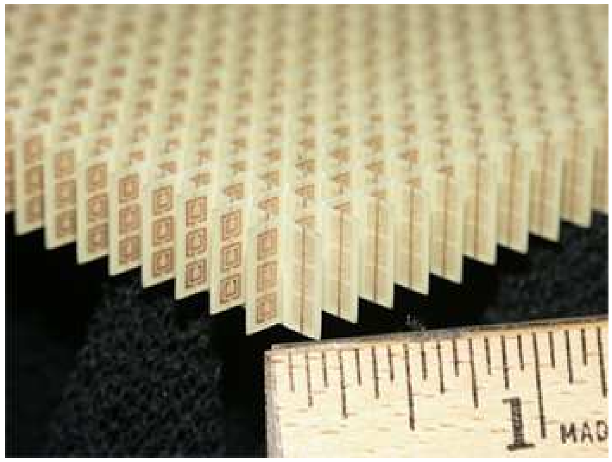

Figure 3.10: Split Ring Resonator array : 1-D square design

- There is the 1-D Split-Ring Structure with two square rings, one inside the other. One set of cited "unit cell" dimensions would be an outer square of 2.62 mm and an inner square of 0.25 mm. 1-D structures such as this are easier to fabricate compared with constructing a rigid 2-D structure.[14] This structure is shown in Fig. 3.4.

- The Symmetrical-Ring Structure is another classic example. Described by the nomenclature these are two rectangular square D type configurations, exactly the same size, laying flat, side by side, in the unit cell. Also these are not concentric. One set of cited dimensions are 2 mm on the shorter side, and 3.12 mm on the longer side. The gaps in each ring face each other, in the unit cell. [14]

- The Omega Structure, as the nomenclature describes, has an Ω-shaped ring structure. There are two of these, standing vertical, side by side, instead of laying flat, in the unit cell. In 2005 these were considered to be a new type of metamaterial. One set of cited dimensions are annular parameters of R = 1.4 mm and r = 1 mm, and the straight edge is 3.33 mm. [14]

- Another new metamaterial in 2005 was a coupled "S" shaped structure. There are two vertical "S" shaped structures, standing vertical, side by side, in a unit cell. There is no gap as in the ring structure, however there is a space between the top and middle parts of the S and space between the middle part and bottom part of the S. Furthermore, it still has the properties of having an electric plasma frequency and a magnetic resonant frequency. [14]

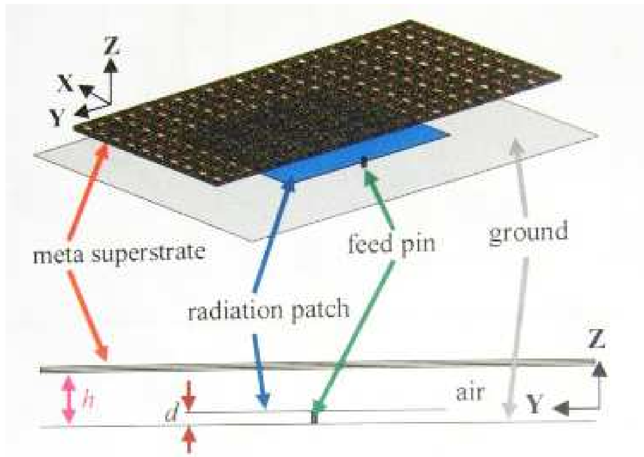

Figure 3.11: Configuration of the S-shaped metamaterial antenna

3.5 The S-shaped metamaterial

A metamaterial substrate, composed of S-shaped split ring resonators, can modify the radiation pattern and exhibit gain enhancement functionality.

3.5.1 Design

Based on principle of the SRR layers, the S-shaped metamaterial has been proposed. It contributed gain enhancement for lower-GHz frequencies.[15]

Fig. 3.11 shows the shematic configuration of the proposed antenna.

The antenna (radiation patch) is centered regarding the 70mm-by-136mm ground plane. It is fed in its middle (feed pin) and is placed at a distance d=4.5mm above the ground plane.

The substrate in between is air ($\varepsilon_r = 1$). The whole structure is covered by a metamaterial plate (meta-substrate). The unit cell of this metamaterial is detailed n Fig. 3.12

Traditionally an enhancing superstrate is a high dielectric constant material and it is placed halfwavelength above the ground plane (h=0.5λ) to meet the resonant condition. [15]

But, for mobile phone applications, half-wavelengthi is unacceptable. For WiMax application for instance, half-wavelength is about h=58mm which is way too big for low-profile requirement. By using a metamaterial plate, a negative reflection phase is provided [15] and the height is reduced to h=10.5mm (h=0.99λ)

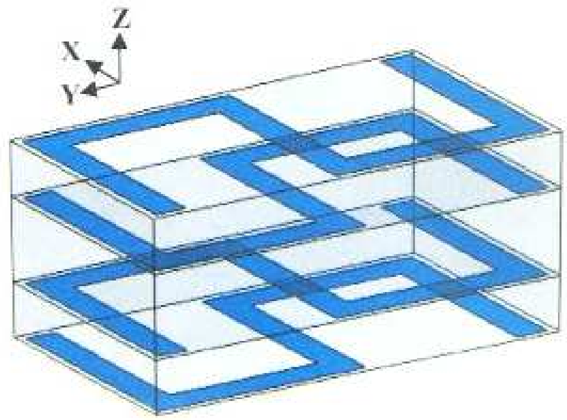

Figure 3.12: Meta unit cell

3.5.2 Measured results

The measurements proved a 390 MHz bandwidth for the WiMax frequency band, but a poor matching : $|s_{11}|_{2.65GHz}$= -13 dB.[15]

The gain is improved a 1.8 dB bringing the maximum gain up to 12.2 dBi.[15]

The experimental results are shown in Fig. 3.13 [15]

3.5.3 Conclusion

The S-shaped split ring resonator metamaterial improved the gain of the resulting antena by 1.8 dB, boosting the maximum to 12.2 dBi. Also the prototype is low-profile and matches with the WiMax frequency. But matching is poor and the resulting efficiency haven't been tested.

3.6 Metamaterial-inspired structures

By metamaterial-inspired, it is meant that the resistive and reactance matching is achieved not with a metamaterial medium but rather with an element such as an inclusion that has or could be used in a metamaterial unit cell design to realize a DNG medium.[1]

The S-shaped metamaterial presented earlier (Fig. 3.12) has a unit cell composed by four layers of "S" and "inverted-S" metallic structures. Taking out one of them and studying it apart and even treating it like a metamaterial itself brought up the Z antenna.

The Z antenna will be presented, which can be considered as the unit cell of the S-shaped metamaterial.

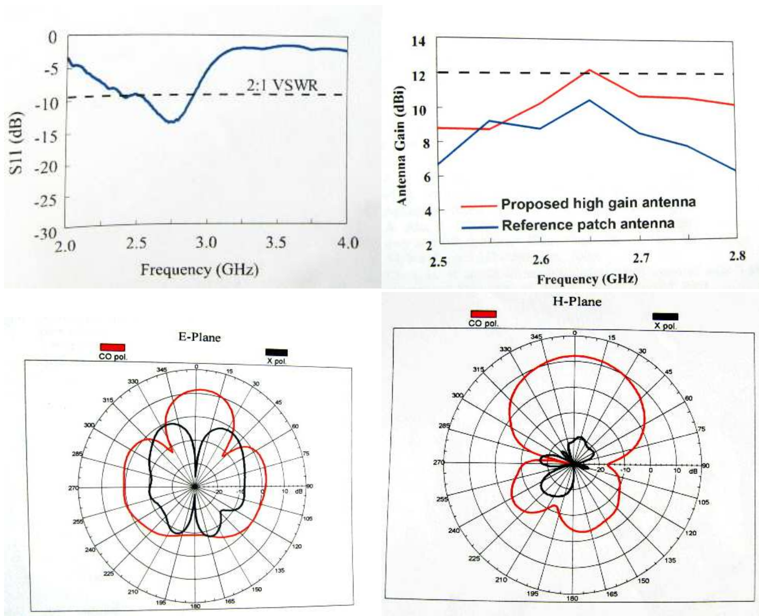

Figure 3.13: Experimental results [ref]

3.6.1 The Z antenna

The Z antenna introduces a metamaterial-inspired structure that is placed in the very near field of the radiating element to achieve complete matching of the resulting antenna to the source. [16]

3.6.2 Problem definition

Typically, the input impedance of an electrically small radiator is characterized by a large reactance and a low radiation resistance [16]. So, to achieve an efficient radiator, an external matching circuit is needed. It will provide the necessary complex conjugate reactance to cancel the antenna one and reach a total input reactance of zero. But these external matching circuits imply losses, then less power to be radiated by the antenna. To avoid the losses, a « natural » matching circuit has been considered. « Natural » is used for meaning that the matching doesn't require an external circuit.

3.6.3 Metamaterial-inspired

The Z antenna is composed by an electrically small radiator and a parasitic Z-shaped element placed in his near field.

The parasitic structure is not metamaterial itself ; but it is inspired by that possibility, i.e., when it is treated instead of a unit cell, the resulting

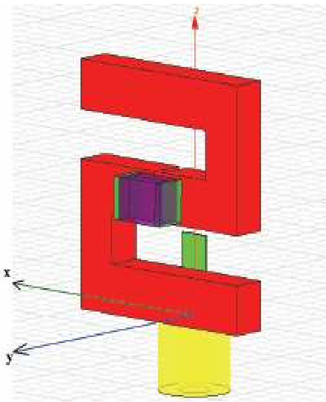

Figure 3.14: The Z antenna

metamaterial exhibits the ε-negative or μ-negative behavior, or both, needed to achieve the resonant interactions essential to the metamaterial-based antennas. [16][17]

3.6.4 Z antenna design

The Z antenna geometry is shown on Fig. 3.14. It consists of a monopole that is printed on one side of a copper sheet. On the other side, there is two split « J's » that are connected by a lumped element inductor. It forms the Z-shaped parasitic element. [18]

The whole structure is placed perpendicularly and in the middle of an (infinite) ground plane as shown in Fig. 3.15.

The improvement of the matching happens when the resonance frequency of the Z element equals the one of the monopole.

The strength of this design is that for tuning the inductance of the Z element to achieve complete matching it is enough to tune the inductance value of the lumped element instead of changing his length, thickness and height.

All the frequency designs can be made by just changing the inductor value and the height of the monopole antenna.[16]

3.6.5 Results

- The minimum |s11| values achieved were all below -40dB at the resonant frequency.
- The maximum overall efficiency reached is 93.42%, for a resonance frequency of 610MHz.[16]
- The maximum gain obtained is 1.61 dB

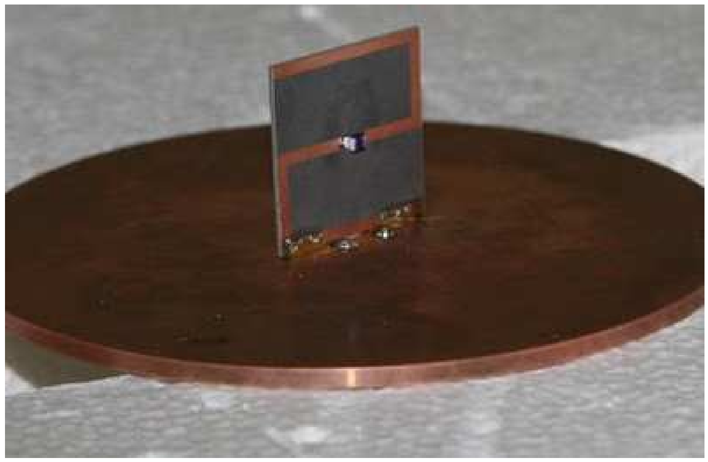

Figure 3.15: Z antenna prototype

3.6.6 Conclusion

The electrically small Z antenna provides nearly complete matching with no external matching circuit.

These antennas are much more efficient than an externally matched monopole antenna of similar size.

The resonance of the antenna can be tuned from the low end of the VHF band to the high end of the UHF band by simply changing the inductor value and readjusting the length of the monopole.

The quality factors indicate an effective use of the antenna volume.

The bandwidths are very small and may not be useful for many practical applications.

One important issue is to consider the lumped element itself not as a circuit element but as an electromagnetic object.

[16] [18]

3.6.7 Advantages for mobile phones

The company Rayspan exhibits new metamaterial antennas for mobile phone applications with unusual properties.

They claim that their metamaterial solutions will displace conventional antennas and RF components and enable a true next-generation of extremely high performance mobile terminals.

They say to be able to bring to the market [19] antennas that can be tuned and re-tuned without the need to rebuild the PCB or remounts components. Indeed multiple tuning elements are added to the original structure to provide means for tuning the resonant frequencies. The resonant frequencies can be shifted by changing the value of an existing resistor and an existing inductor.

Also their antennas are ultra-compact in size while offering equal or better performance. The return loss goes until -25dB at 900MHz and -15dB at 1,8GHz. The efficiency is equal to 0,45 and 0,55 for frequencies respectively.

Reduced SAR values are other advantages offered by their metamaterial antennas.

Chapter 4

SIMULATION RESULTS : Z antenna for handsets presentation

In order to have a better understanding of the new properties offered by the metamaterials to the small antennas and to find new possible designs, with better characteristics, simulations have been done. The simulations have been run with the parallel Finite Difference Time Domain (FDTD) developed at the Antennas, Propagation and Radio Network-ing group at Aalborg University.

In this chapter is presented one of the last and most successful simulation. All the other simulations that have been run to lead to this final version are presented in the appendix 1 and 2. The proposed designs started from a reproduction of the Z antenna described in the paper [16] (antenna structure in the middle and perpendicular to a phone ground plane) and changed until a design that fits with handsets requirements (a typical ground plane and the radiating element on the top). This design is presented below.

4.1 Computation of the results

4.1.1 Requirements

In order to be more realistic, the following parameters have been chosen :

- Length of the phone : 100mm
- Length of the ground plane : 90mm
- Width of the phone : 40mm
- Battery (PEC) : 40x40x10 mm
- Space left for the antenna : 40x10x10 mm

This is represented in the scheme in Fig. 4.1:

The domain boundaries have been chosen to be large enough for considering that after a reasonable time, the energy inside the domain is below a threshold.

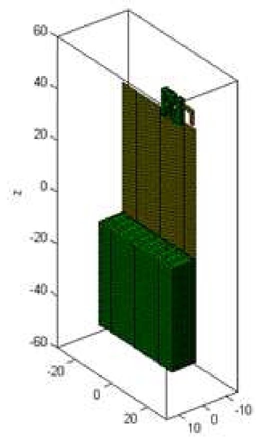

Figure 4.1: Requirements for designing small antennas

Domain boundaries : 60x30x120 mm

In this domain (assumed to be perfectly matched), the termination conditions are :

- Maximum number of time steps : 80 000
- Total energy below : -60 dB

4.1.2 FDTD

The Finite-Difference Time-Domain (FDTD) method has been proven to be one of the most effective numerical methods in the study of metamaterials. [20]

It is widely used because it is simple to implement numerically. It provides a flexible means for directly solving Maxwell's time-dependent curl equations by using finite differences to discretize them. Since it is a time domain solver, it is convenient for dealing with the characteristics of metamaterials over a wide frequency band. The FDTD algorithm, as proposed by Yee in 1966, is second-order accurate in both time and space. Numerical stability of the Yee algorithm requires that we set an upper bound on the time step (Δt) that is determined by the spatial increment Δx, Δy and Δz. [20]

More details in appendix 3.

The parameters used to compute the FDTD method are :

- Cell size : 1 mm
- Frequency resolution : 1MHz

4.1.3 Fyrkat

The simulations that will be computed are contained in files that can weight up to 1 050 MiB. To run this simulations more than one processor is needed and a lot of memory as well. Therefore, the simulations have been run on the "Fyrkat", which is a supercomputer of 70 nodes ; each node has 8 processors , and each processor has 2 Giga Bits of memory. For each simulation, the appropriate number of node and processor has been chosen.

4.2 Parameters to analyze

One starting design will be picked, and many simulations will be run on it, in order to see the impact of :

4.2.0.1 With one Z element

- Distance from the Z element to the antenna
- Distance from the Z element to the ground
- Distance from the Z element to the source
- Size of the Z
- Width of the Z
- 3D or 2D
- Impact of the battery
- Influence of an additional permittivity layer ,

all compared with the starting design and with the monopole alone (without the Z element).

4.2.0.2 With two Z elements

- Adding a second Z element
- Distance between these two Z to the antenna

4.2.0.3 By adding a coil on the Z element in order to tune it

Let's see first the proposed design, on which the changes will be made and analyzed.

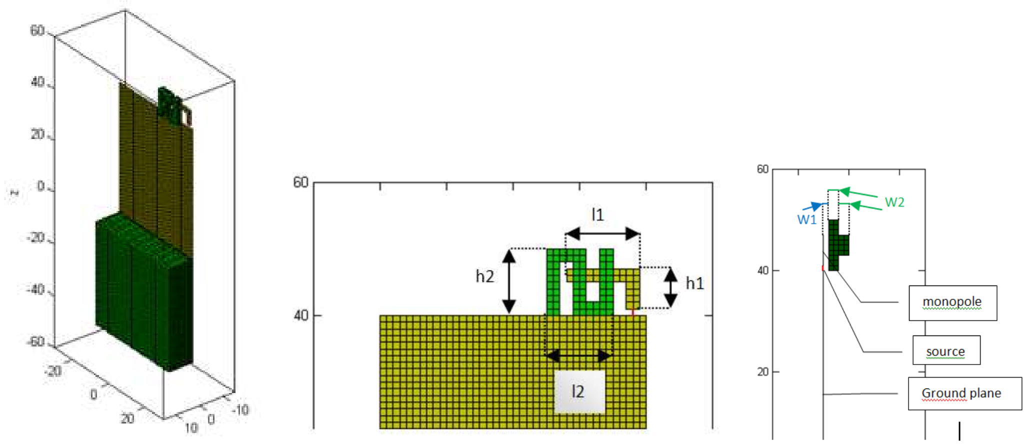

Figure 4.2: Starting design

4.3 Starting design

4.3.1 Parameters

The first parameters (size of the Z element, length of the monopole, distance between the Z and the monopole) have been chosen according to a paper about Z antenna experiments in a way that the resulting antenna fits with the phone requirements.

Also, the most important difference with the paper's design [16] is that the Z element is detached from the ground plane.

Fig. 4.2 is a picture of the modelized antenna :

The parameters are resumed in the following table :

sizes	mm
h1	7
l1	11
h2	10
l2	6
w2	2
w1	1

The source is placed at 2 mm from the edge of the ground plane. The Z element starts at 5 mm from the same edge.

h1 stands for the height of the monopole and l1 stands for the length of the horizontal part of the monopole.

h2 stands for the height of the Z element, l2 for the lenght of each "J" forming the Z.

w2 stands for the width of the Z element and the width of the coil.

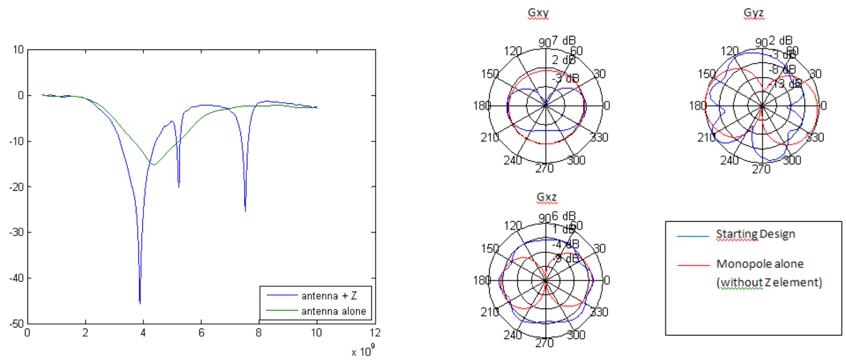

Figure 4.3: left: |s11|(dB) vs f(Hz) for the same antenna with and without the Z element. right: gain comparison between the Z antenna and the monopole itself

w1 stands for the distance between the monopole and the Z element.

4.3.2 Results

In Fig. 4.3 can be seen the s_{11} parameter of the starting design. This graph shows three resonance frequencies, the first one being the best regarding the matching. The values are resumed in the following table:

	f_{r1}	f_{r2}	f_{r3}
GHz	3.9	5.2	7.5
s_{11}(dB)	-45	-20	-25
BW(GHz)	2	0.3	0.5

4.3.3 Comparison with the monopole alone

The s_{11} and the gain of the whole structure (antenna + Z element) and of the antenna alone are compared in Fig. 4.3

It can be observed that addind the Z element highly increases the matching of the antenna structure and shifts it 0.4 GHz lower.

The radiation patterns of the Z antenna and the monopole alone are compared in Fig. 4.4. In the radiation pattern and the gain of the monopole itself the phone acts like a dipole, as could be expected. The Z antenna pattern is more complex.

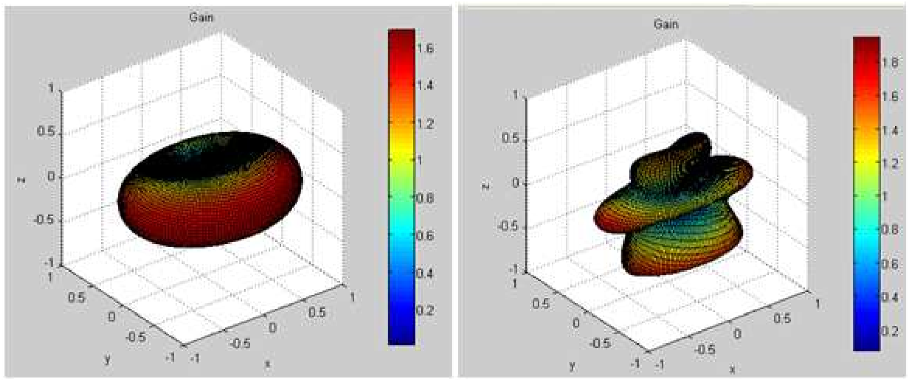

Figure 4.4: Radiation patterns (left:monopole alone acting like a dipole, right:Z antenna)

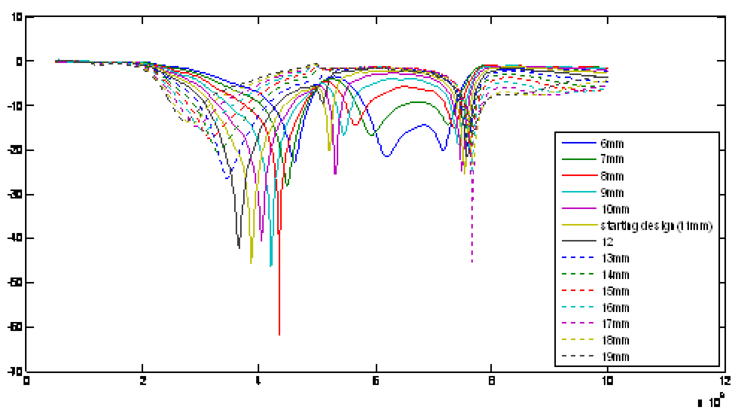

Figure 4.5: Representation of the |s11| when the length of the monopole varies

4.4 Changing the monopole length

Many simulations have been run with the lenght l1 of the monopole as variable. l1 is increased, one millimeter by one millimeter, from 7mm long to 20mm long.

4.4.1 Results

In Fig. 4.5 are presented the results regarding the s_{11} parameter.

The results are summarized in the following table :

	l1=6mm	l1=7mm	l1=8mm	l1=9mm	l1=10mm	l1=11m	l1=12mm	l1=13mm	l1=14mm	
f_{r1}(GHz)	4.6	4.5	4.3	4.2	4.0	3.8	3.6	3.4	3.2	
s_{11}(dB)	-22	-27	-61	-45	-40	-45	-42	-26	-20	
BW(MHz)	1100	1500	1750	2000	2000	2000	1900	1800	1700	
	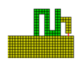		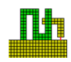	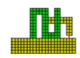			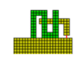	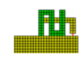		

	l1=15mm	l1=16mm	l1=17mm	l1=18mm	l1=19mm
f_{r1}(GHz)	3.1	3	2.9	2.8	2.7
s_{11}(dB)	-17	-15	-14	-14	-13
BW(MHz)	1500	1500	1400	1400	1200
	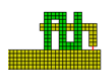				

Note that:

- the monopole is crossing the right part of the Z element when l1=7mm.
- the monopole is crossing the middle part of the Z element when l1=11mm.
- when the length of the monopole is greater than l1=14mm, the monopole crosses the left part of the Z element.

4.4.2 Conclusions

First, we can observe that, as expected, the longer the monopole , the lower the resonance frequency. The presence of the Z element doesn't change this. Each step of 1mm correspond to a reduction in the resonance frequency of 0.2 GHz.

Also, the minimum of the s_{11} depends even on the coupling between the Z element and the monopole ; in other words it depends on where the monopole stops regarding the length of the Z element. When the length of the monpole is greater than the length of the Z element, there is no matching anymore ($s_{11} < -20dB$).

It is said in [16] that the perfect matching occurs when $f_{reso(Z)} = f_{reso(monop)}$, then when l1 changes, the resonance frequency of the monopole itself changes ; but not the one of the Z element. Therefore in order to keep this equality between resonance frequencies, the parameters of the Z element (sizes, width, etc.) should be modified . This point will be discussed in the coil simulations. [section 5]

4.5 Changing the distance between the Z element and the monopole

The variable that is analyzed in this section is w1. w1 varies from 1mm to 6mm with one millimeter step.

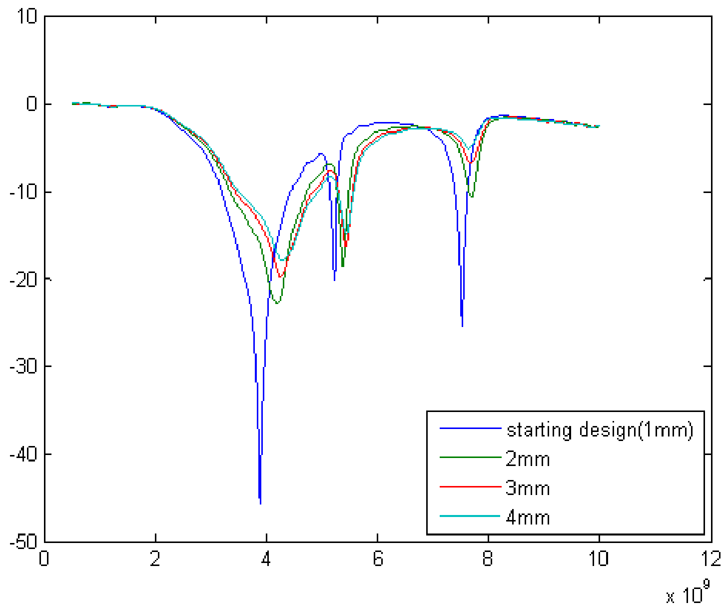

Figure 4.6: |s11| parameter when the distance between the monopole and the Z element varies

4.5.1 Results

The s_{11} results are presented in Fig. 4.6

4.5.2 Interpretation of the results

It can be observed that the matching is decreasing when the Z element moves away from the antenna. The first millimeter step already has a strong influence on the matching, moving the s_{11}depth from $s_{11} = -45dB$ to $s_{11} = -23dB$. It is getting worse as w1 increases.

Also, the resonnance frequencies become higher.

4.5.3 Conclusion

When the distance increases, the coupling between the Z element and the antenna decreases. Then the matching goes worse and the f_r moves up.

The formula $f_r = \frac{1}{2\pi\sqrt{LC}}$ [16] can be applied and confirms that when the coupling decreases (LC decreases), the resonance frequency increases. This formula will be used to determined the value of the coil in the section 5

The closest the Z element from the antenna, the best the coupling and the matching.

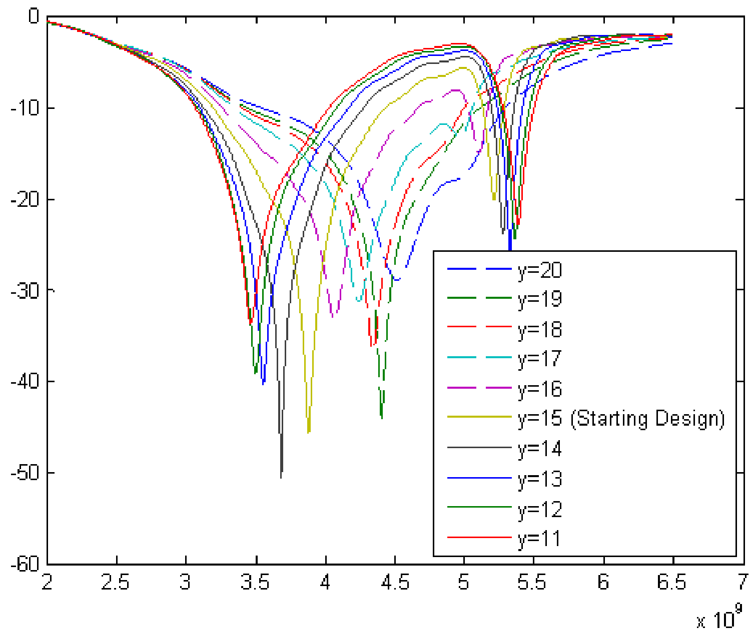

Figure 4.7: |s11|(dB) vs frequency (Hz) while moving the Z element closer or further from the source

4.6 Changing the distance between the Z element and the source

4.6.1 Design

In the starting design the Z element is placed about the middle of the monopole. But it could be shifted to right or the left until 6mm in each side. These designs have been made and run and the |s11| parameter analyzed.

4.6.2 Results

The s_{11} parameter (values in dB) versus the frequency is presented in Fig. 4.7. The "y" variable stands for the right end of the Z element. When "y=20", it means that the Z element is placed at the right edge of the ground plane. Then, the projection of the right side of the Z element coincides with the source. When "y" decreases, the Z element is sliding to the left until that the projection of the end of the Z coincides with the end of the monopole: "y=13".

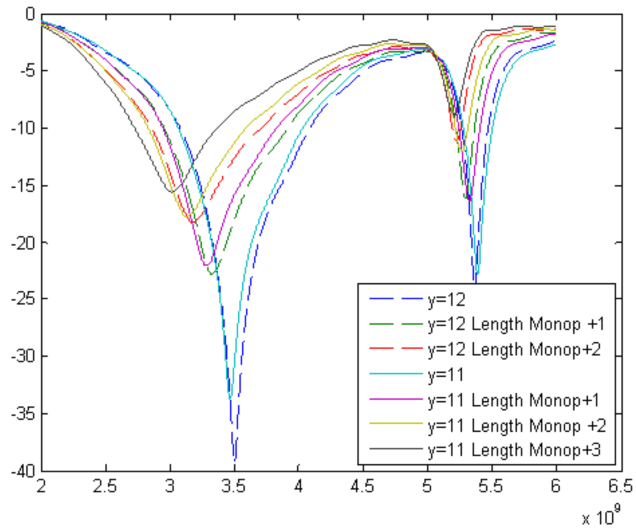

Figure 4.8: Shifting the Z element further form the source and adding length to the monopole

4.6.3 Conclusion

From the Fig. 4.7, it can be shown that as the Z element is going further from the source, the resonance frequency goes lower. The best matching position are for "y=14" and "y=19", which corresponds to the position where the end of the monopole is crossing the vertical arm of the Z element. These results add strength to the assumption done in 4.4.2 saying that the matching depends on the relative position of the Z element respect to the monopole.

When the Z element is going further than the end of the monopole ("y=13", "y=12" and "y=11"), the resonance frequency is not shifted anymore, and just the matching get worse.

Therefore, is it possible to go even lower in frequency by adding length to the monopole and shifting more the Z element? These new results are showed in Fig. 4.8.

This experience doesn't show any better result, while the monopole is longer, the |s11| is going above -20dB. Then it appears to be a threshold and the resonance frequency cannot be shifted more than 1 GHz.

This confirms another assumption saying that the resonance frequency of the Z element depends on its parameters. Therefore they will have to be modified to get lower frequencies. This point will lead to a discussion in 5.

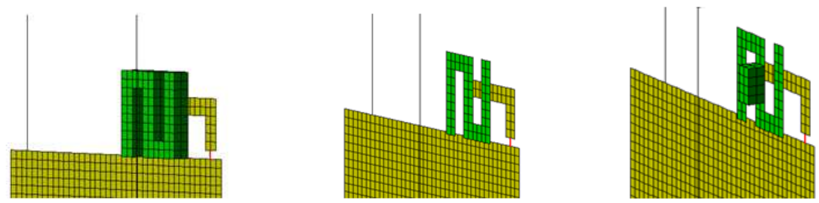

Figure 4.9: 3D and 2D designs. left : full Z in 3D, middle : full Z in 2D, right : two 2D "J"'s and a 3D coil

4.7 3D vs 2D

In this section, will be compared the starting design with :

- a full Z by removing the coil (2mm width)
- a full 2D Z without coil (1mm width)
- a 2D Z with a 3D coil (2mm width)

This three designs are presented on Fig. 4.9 :

4.7.1 Results

The s_{11}parameter of these designs is compared on the Fig. 4.10

4.7.2 Conclusion

The Z-shaped element is built with two J-shaped layers, joined with a coil on the top of them. The structure of the Z element is fully detailed in 3.6.4.

Removing the coil and replacing the two "J"s by a full "Z" doesn't make any big change in the shape of the s_{11}.

But, the two 2D models have a non acceptable matching to the source (above -20dB). Acceptable minimum was defined in [16].

Since "metamaterial" is an appelation for a **medium**, it seems expectable that the 3D model acts better.

4.8 Adding a second Z element

4.8.1 Design

The structure of the starting design includes the monopole, one millimeter space, the Z element and the coil ; which represents 4mm thickness. To fit with the requirements of the phone, there is juste the space to add another Z element, with another one millimeter distance. The design is presented in the Fig. 4.11. The whole antenna structure is now occupying the 10mm allowed for the thickness.

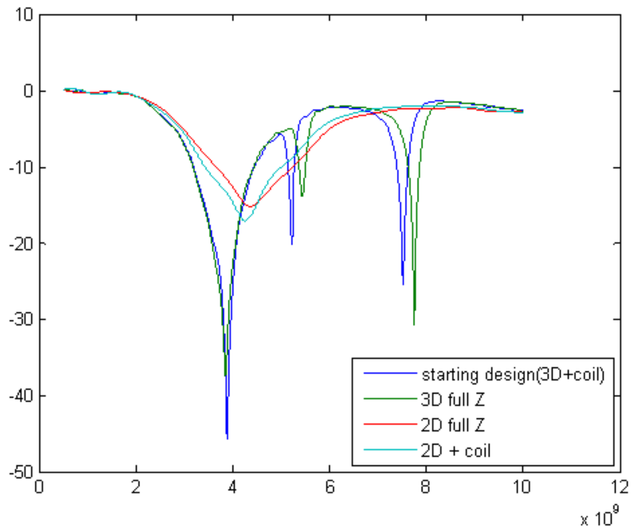

Figure 4.10: |s11| parameter when the width of the Z element changes

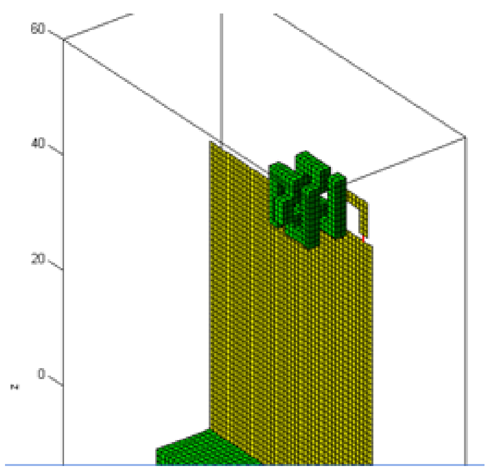

Figure 4.11: Design with two identical Z elements

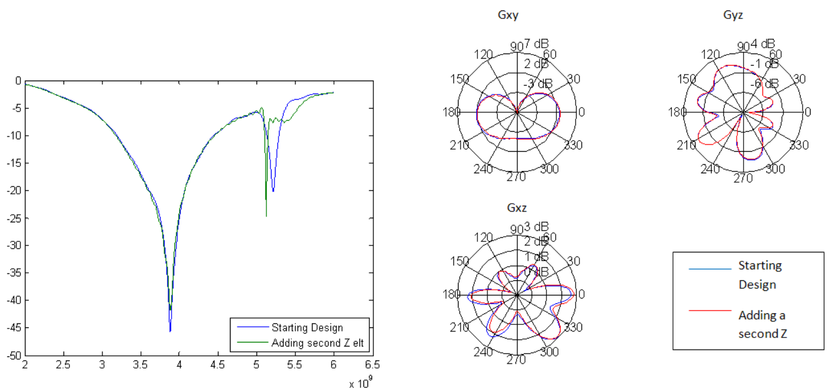

Figure 4.12: On the left : |s11| (dB), on the right : gain (dB) for the starting design and the two Z elements design.

4.8.2 Result

The new |s11| parameter has been analyzed and compared with the one of the starting design. The result is presented in Fig. 4.12.

Adding a second Z element doesn't improve the matching or changes the resonance frequency in this case.

The gain of the starting design and the two Z designs is also plotted on Fig. 4.12.

The two gains are very similar except in the Gxz plane, where there is less than half dB difference.

Adding a second Z element does not improve the characteristics of the resulting antenna.

4.9 Changing the feeding

In the starting design only the monopole is fed and it is separated from the Z element with 1mm free space. What about feeding only the Z element or feeding both the monopole and the Z element? In order to answer this question, the appropriate wires have been added to the design and new simulations have been run. The |s11| parameter is presented in Fig. 4.13

The best matching is obtained when both the monopole and the Z element are fed but this change implies going 0.4 GHz higher in frequency and sacrifying bandwidth. When only the Z element is fed, there is not distinguishable resonance.

Feeding only the monopole appears to be a good compromise.

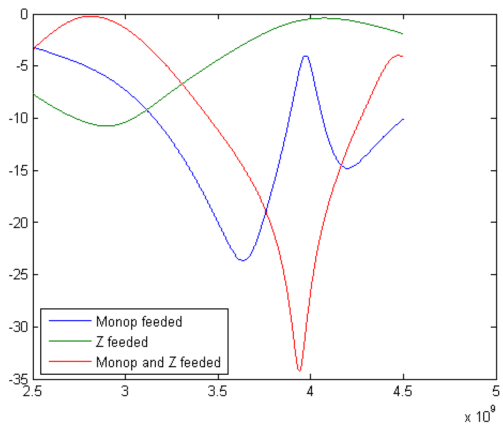

Figure 4.13: Changing the feeding

4.10 Changing the permittivity

The starting design shows a Z element and a monopole, one millimeter distant. Both are in free space, which means that the relative permittivity is equal to one ($\varepsilon_r = 1$). This space between the Z and the monopole has been fill with a small 12x10x1mm layer. And the effect of its relative permittivity has been analyzed.

4.10.1 Design

Fig. 4.14 shows the design with a layer in between the two elements of the antenna structure. Its permittivity has been changed from 1 to 60.

4.10.2 Results and Conclusion

The |s11| parameter is shown on Fig. 4.14

Increasing the permittivity allows to go lower in frequency but means sacrifying the bandwidth. Any good compromise has been found.

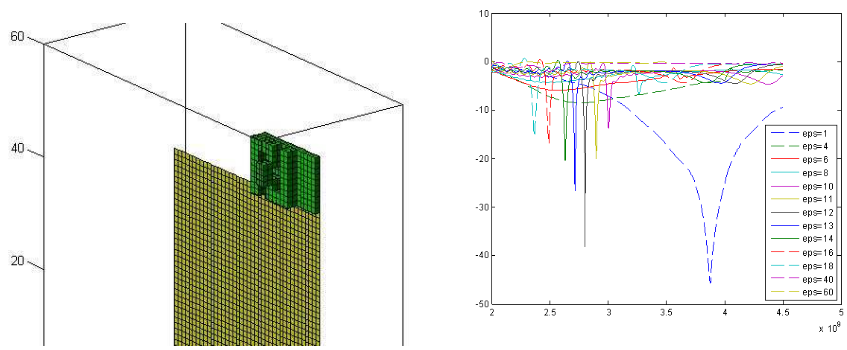

Figure 4.14: On the left, the design : layer (with variable permittivity) inserted in between the Z element and the monopole. On the right, the results : Influence of increasing the permittivity in the space between the Z and the monopole on the |s11| parameter

Chapter 5

SIMULATION RESULTS : Tuning the Z antenna

The resonance frequency of the starting design is 3.9GHz, which is very high for mobile devices applications. The aim of this section is to low the resonance frequency of the resulting antenna (monopole and Z element). One way to do it would be to change the parameters (sizes, width, etc.) of the Z and of the monopole but this way is not so straightforward and can be very long, overall for the Z structure. It will be explained and shown below how the resonance frequency of the Z element is dependent on the value of its overall inductance and how it can be lowered by simply changing the value of the inductance of the coil on the top of it.

5.0.3 Theory

First, the value of the coil in the starting design has to be determined.

To determine the inductance of a PEC layer coil, the following formula will be used [21] :

$$L = l(ln\frac{4l}{d} - 1) * 200 * 10^{-9} \tag{5.1}$$

where :

l is the length of the coil (m)

d is the diameter of the coil (m)

So, in the starting design (l=4mm and d=1mm), $\mathbf{L_{3.9} = 0.863}$ **nH.**

The value of the inductance of the two “J’s” (i.e. without the coil on the top) is assumed to be neglictible in comparison with the inductance of the coil, as said in the paper [16].

The capacitance of the Z element itself can then be determined by [16] :

$$f_r = \frac{1}{2\pi\sqrt{LC}} \tag{5.2}$$

used at f_r= 3.9 GHz.

Then, in the starting design, $\mathbf{C = 1{,}950\ .10^{-12}\ F.}$

It can be easily seen that by increasing the value of the inductance L, the resonance frequency will be lowered.

To achieve the license-free band $f_r = 2.45$ GHz, the inductance should be : $\mathbf{L_{2.45} = 2.16\ nH.}$

This value of inductance can be reached with the layer PEC, but since it is a "ln-formula", the increase of inductance is very small compared to the increase of length needed. In fact, L = 2.16nH leads to a 20mm long layer. This structure does not fit with the requirements of handsets devices.

Therefore, the coil will be realized with a wire turning around a high permeability layer. This kind of coil can be tuned by changing only the value of the permeability layer inside. The inductance will be determined by the following formula:

$$L = \frac{\mu N^2 A}{l} \tag{5.3}$$

where :

A is the cross sectional area (cm^2)

l is the solenoide length (cm)

N is the number of turns and the coil radius

μ is the permeability.

Because of the parameters for the FDTD simulations and the frequency range, the value of the permeability cannot exceed $\mu = 100$.

The value of the inductance of the two "J"s element is assumed to be neglictible regarding the inductance of the coil [16]. The value of the capacitance as well.

5.0.4 Simulations

5.0.4.1 With a wire coil : 4 turns

The PEC layer in the starting design has been replaced by a wire coil of the same dimensions. The relative permeability of the layer inside the coil has been changed from 1 to 10 in order to change the total inductance.

Increasing the inductance permits to decrease the resonance frequency, as predicted in the theory. The Fig. 5.2 shows the relative decrease of the resonance frequency with respect to the increase of the permeability of the layer inside the coil, which increases the inductance of the coil and therefore of the Z element.

A threshold is reached and increasing the value of the permeability does not permit to go below 3.2 GHz. This value is determined by the number of turns.

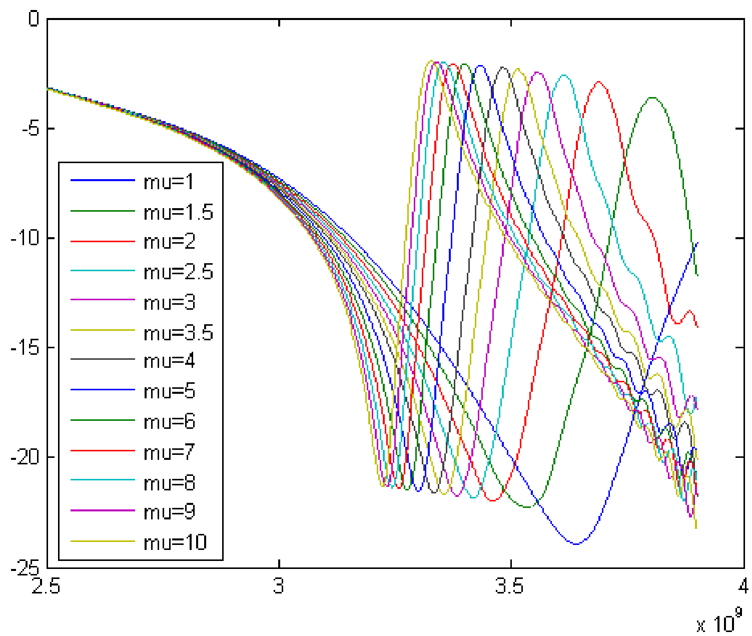

Figure 5.1: |s11|(dB) while changing the inductance of the coil on the top of the Z element. mu stands for the relative permeability of the layer inside the coil. (four-turns wire coil)

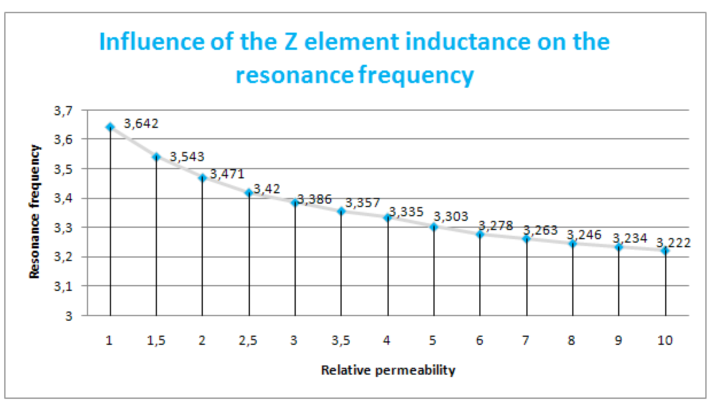

Figure 5.2: Refonance frequency tendance when the permeability (then the Z element inductance) increases. (four-turns wire coil)

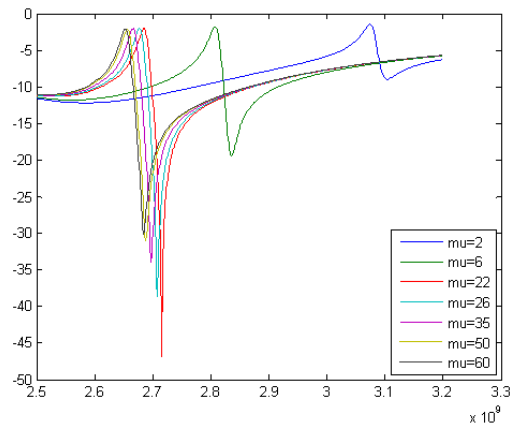

Figure 5.3: |s11|(dB) while changing the inductance of the coil on the top of the Z element. mu stands for the relative permeability of the layer inside the coil. (six-turns wire coil)

5.0.4.2 With a wire coil : 6 turns

The inductance is highly dependent on the number of tunrs of the wire, as shows the formula above. To decrease even more the resonance frequency, the number of turns has been increased from 4 to 6.

New simulations have been run with a six-turns wire coil and a permeability varying from 2 to 60. The results are presented in Fig. 5.3.

Again, the variation of the resonance frequency reaches a threshold that cannot be passed by increasing more the value of the permeability. The lowest resonance frequency obtained is about 2.65 GHz.

5.0.4.3 Conclusion

By increasing the number of turns, lower frequencies can be reached but the mobile phone requirements does not afford the needed volume to reach 2.45 GHz, or 1.8 GHz.

The 6-turns model with $\mu = 60$, leads to an inductance L = 1.66 nH and a resonance frequency f = 2.68 GHz. This values correspond to the LTE frequencies.

A reduction of 1.2 GHz was obtained by simply changing the value of the coil and increasing the length of the monopole. Any big change in the antenna structure was necessary.

To reach the unlicensed frequency f = 2.45 GHz, the inductance needed is L = 2.16 nH.

5.0.5 Selected designs

After running all the tuning-simulations three designs have been selected : one for the LTE band (∼ 2.6 GHz), two for the license-free band (∼2.45 GHz ; WiFi, Bluetooth, etc.).

They are presented below.

5.0.5.1 The Height-turns wire coil design

The lowest resonance frequency achievable by adding a coil on the top of the Z element is **f = 2.68 GHz**. The coil is composed by a μ_r= **40** layer and a wire **8 times turned** around. This configuration lead to **L = 1.60 nH**. The length of the monopole had to be adjusted. The length equals **26mm**. (The 6 first millimeters on the source side are folded). The corresponding design, |s11| parameter (dB) and gain (dB) are presented on Fig. 5.4

The bandwidth at -6 dB is **400 MHz** (from 2.23 GHz to 2.65 GHz) for the first resonance but doesn't present a good matching while the bandwidth of the second resonance is narrower : **300MHz** (from 2.67 GHz to 3.00 GHz) but has a matching up to - 36 dB.

5.0.5.2 The closer coil design

To get even lower frequencies, the coil must be closer to the monopole in order to get hit more strongly by the fields and be more efficient. Moreover, the monopole should be longer but not further from the Z in order to keep strong fields around the coil. The new structure that is presented in this sub-section might respond to these requirements.

The coil is not anymore on the top of the Z element but in between the two "J"'s that form it. Then, it is **2mm distant** from the monopole instead of 3mm. The monopole is long **30 mm** but the first 6 mm (source side) and the last 5 mm (end side) are folded. The results are presented in Fig. 5.5.

The resonance frequency is **f = 2.48 GHz** but the bandwidth at -6 dB is narrower : **220MHz**. The matching achieves **-25 dB**.

In this configuration the coil is a **six-turns** wire and a μ= **50** layer. Which leads to an inductance **L = 0.7 nH.**

It is interesting to notice that the inductance is smaller than in the previous design but the resonance frequency is lower, just because it is placed closer to the monopole. Since the Z element is not connected to the ground and the source, it only reacts to the E and H fields radiated by the monopole. The closer it is, the stronger they are.

5.0.5.3 The capacitor design

The coil structure cannot get closer to the monopole, neither the Z element. The limitations are physical.

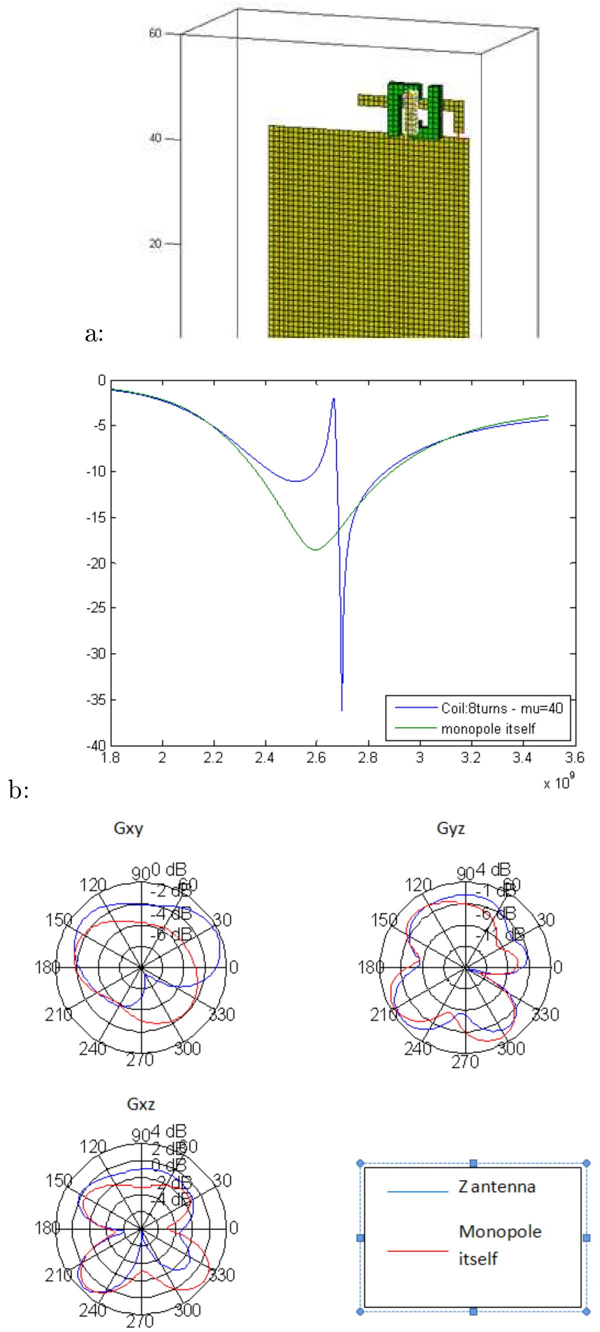

Figure 5.4: a : design ; b : |s11| in dB for the height-turns wire coil antenna design compared to the monopole itself ; c : gain in dB of the Z antenna and the monopole itself

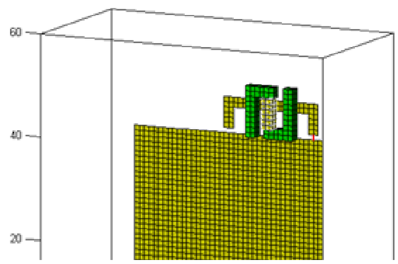

a:

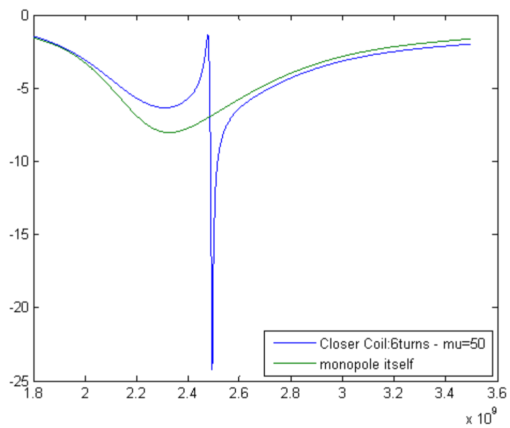

b:

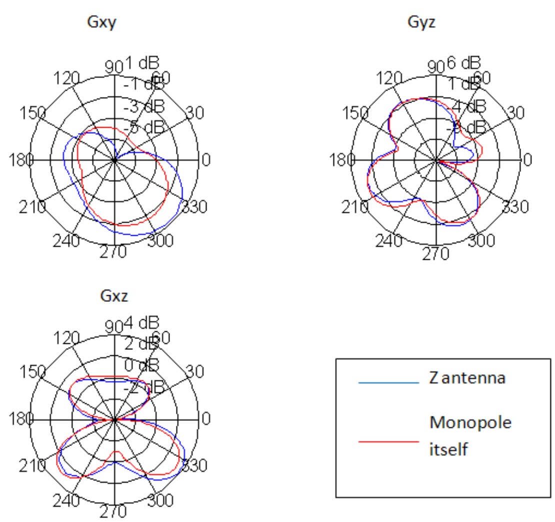

c:

Figure 5.5: a : design ; b: |s11| in dB for the six-turns wire closer coil antenna design compared to the monopole itself ; c : gain in dB of the Z antenna and the monopole itself

To get even lower frequency, the whole design has to be reviewed, re-thought.

From the microwave engineering, it is know that a coil in serial and a capacitor in parallel can act in similar way. What about in the near-field?

Several new simulations have been run, with different capacitances. The best design is presented in Fig. 5.6

The characteristics are summarized in the following table :

f_r	2.44 GHz
$s_{11}(dB)$	-27 dB
BW_{-6dB}	50 MHz
Monopole total length	6+14+6 mm
Capacitor	5 nF
Capacitor length	8mm
Distance capa-monop	6mm

5.0.5.4 Conclusion

A reduction of the resonance frequency of 1.45 GHz could be achieved keeping the same antenna structure. The only changes were in the value of the coil/capacitor and the length of the monopole.

If the same reduction can be kept for all the frequency ranges, then with a different starting design the 1.8 GHz band (high band of the GSM) and the 2.45 GHz band (Bluetooth and WiFi) could be covered with the same antenna, just changing the value of the coil/capacitor. Maybe, even the 900 MHz.

In the next section, the influence of the additional Z element regarding to the user's body will be discussed.

5.0.6 User's influence

The three previous designs have been simulated with hand and head phantoms. The SAM (Specific Anthropomorphic Mannequin) will be used to simulate the user, the hand is the talk mode model.

When a mobile phone is used in close proximity with the human body, it results in a detrimental effect in its communication performances. Also, the way the mobile is hold strongly affects the radiation efficiency and causes radiation pattern deterioration and causes detuning [22].

Absorption loss is more significant than mismatch loss, while the dielectric properties of the phantoms play a minor role [22].

What is really important is what happens in the reactive near-field of the antenna : the index finger and the head. The index finger may absorb more than half of the power [22].

In the previous designs cases, the antenna is directly close to the head, while the index touches the Z element.

a(front view): 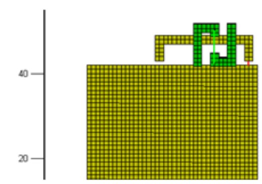

a(side view): 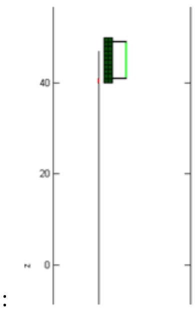

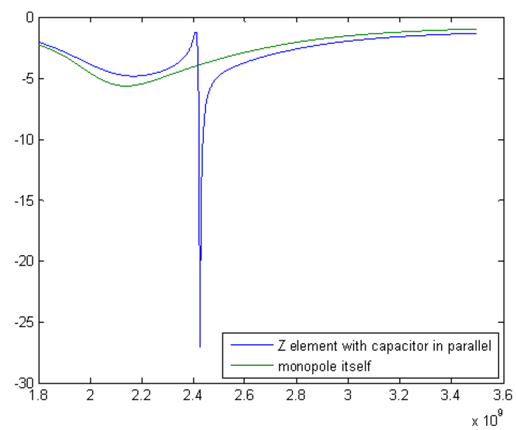

b:

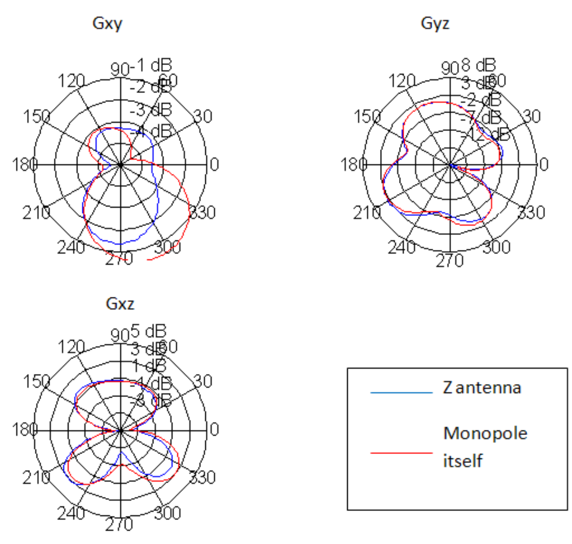

c:

Figure 5.6: a : design (front and side views) ; b : |s11| in dB for the capacitor design compared to the monopole itself ; c : gain in dB of the Z antenna and the monopole itself

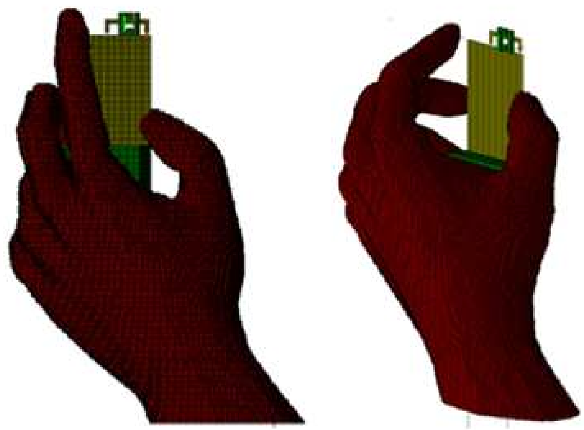

Figure 5.7: Hand phantoms. On the left : the 'firm' grip (H2). On the right : the 'soft' grip (H1).

5.0.6.1 Hand effect

Two grips have been studied : the 'firm' grip and the 'soft' grip. They differ by the position of the index finger and the distance between the palm and the mobile phone. The Fig. 5.7 shows how the handset fits into the modeled hands.

The hand have been placed in such way that the index finger touches the antenna area. It is on the side of the Z element but not close enough to touch it. The other fingers are on the phone battery area, in contact with it. Because of the small size of the antenna, the index finger is not overlapping the Z or the monopole. Therefore, its impact will be reduced.

The exact position of the other fingers is less important since they are not in the immediate near-field of the radiator [22].

The influence of the hand on the antennas as been studied but the results will be presented with the influence of the head also.

5.0.6.2 Hand and Head effect

The head phantom has been added to the 'firm' hand simulations as shown in the Fig. 5.0.6.2.

See Fig. 5.9 for the **"Height turns wire coil Z antenna"**

See Fig. 5.0.6.2 for the **"Closer coil, Six turns wire coil Z antenna"**

See Fig. 5.0.6.2 for the **"Closer coil model"**

5.0.6.3 High permittivity layer effect

Is it possible to counteract the radiation efficiency degradation caused by the human body proximity ? Some tests have been run with a high permittivity

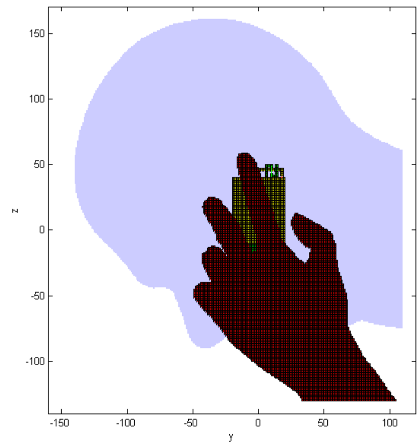

Figure 5.8: Hand and SAM's head phantoms

layer ($\varepsilon_r = 100$) in between the index finger and the antenna structure. A layer: 20mm x 20mm x 1mm with relative permittivity of 100 have been added to the simulations as shown on Fig. 5.0.6.3

The results are shown on Fig. 5.0.6.3 for the three different models.

5.0.6.4 Summarize of the results

The two graphics shown on Fig. 5.0.6.4 summarize all the results found respect to the user's influence. They will be discussed in the following chapter, 6.3.

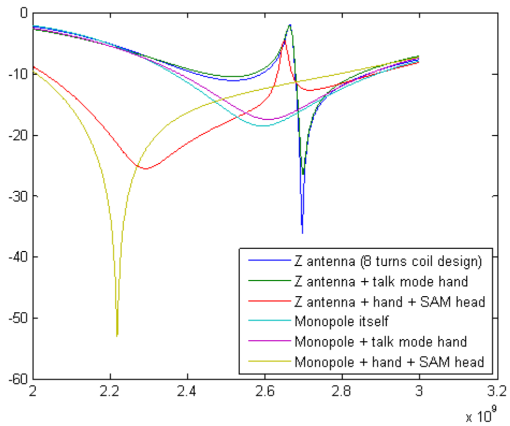

a:

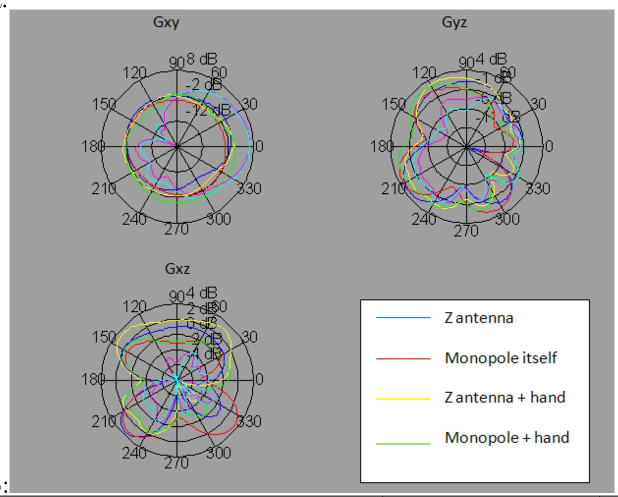

b:

c:

	Z antenna	Monopole itself
efficiency adding a hand and SAM's head	0.20 = -6.99 dB	0.19 = -7.17 dB

Figure 5.9: **Height turns wire coil model** : |s11| (a), gain (b) and efficiency (c) when adding a hand and SAM's head to the "Z antenna" and the "monopole alone" simulations

a: 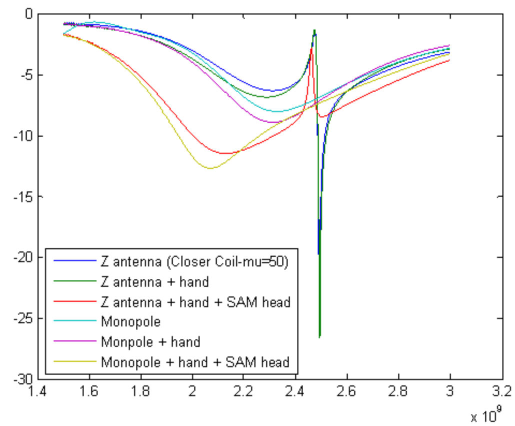

b: 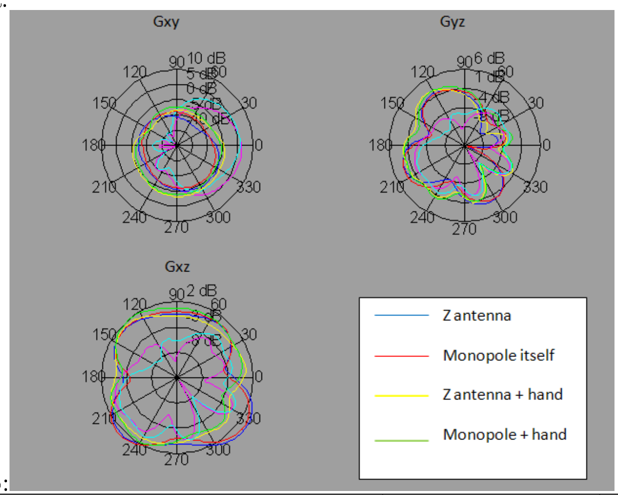

c:

	Z antenna	Monopole itself
efficiency adding a hand and SAM's head	0.20 = -7.00 dB	0.18 = -7.47 dB

Figure 5.10: **Closer coil model** : |s11| (a), gain (b) and efficiency (c) when adding a hand and SAM's head to the "Z antenna" and the "monopole alone" simulations

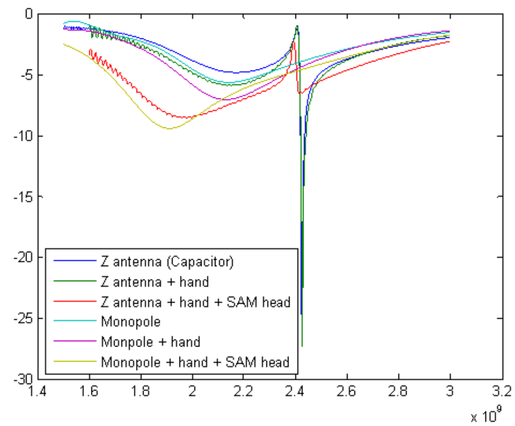

a:

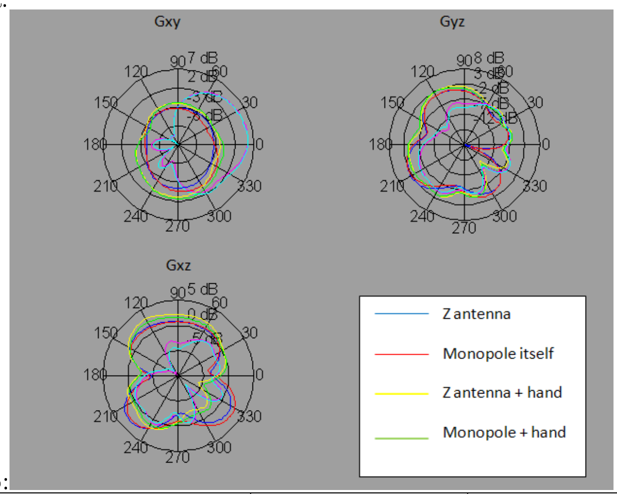

b:

c:

	Z antenna	Monopole itself
efficiency adding a hand	0.17 = -7.60 dB	0.17 = -7.57 dB

Figure 5.11: **Capacitor model** : |s11| (a), gain (b) and efficiency (c) when adding a hand and the SAM's head to the "Z antenna" and the "monopole alone" simulations

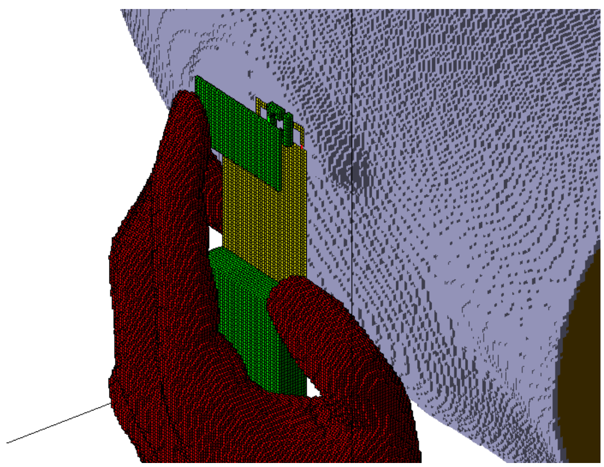

Figure 5.12: Adding a $\varepsilon_r = 100$ layer to try to cancel the deterioration caused by the index finger

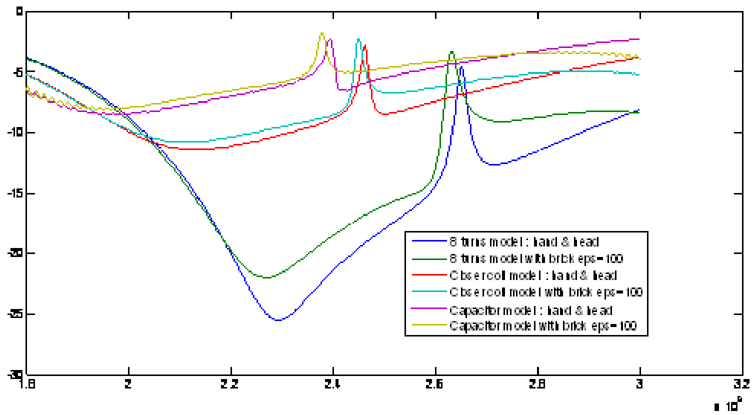

a:

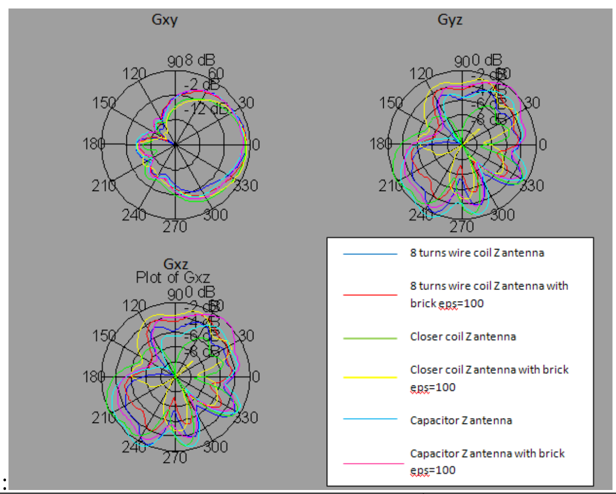

b:

c:

	8 turns wire coil model	closer coil model	capacitor model
efficiency with head and hand	0.20 = -6.99 dB	0.20 = -7.00 dB	0.17 = -7.60 dB
efficiency with head and hand while adding an eps=100 layer	0.26 = -5.85 dB	0.29 = -5.36 dB	0.21 = -6.72 dB

Figure 5.13: |s11| (a), gain (b) and efficiency (c) for each one of the three models adding an $\varepsilon_r = 100$ layer

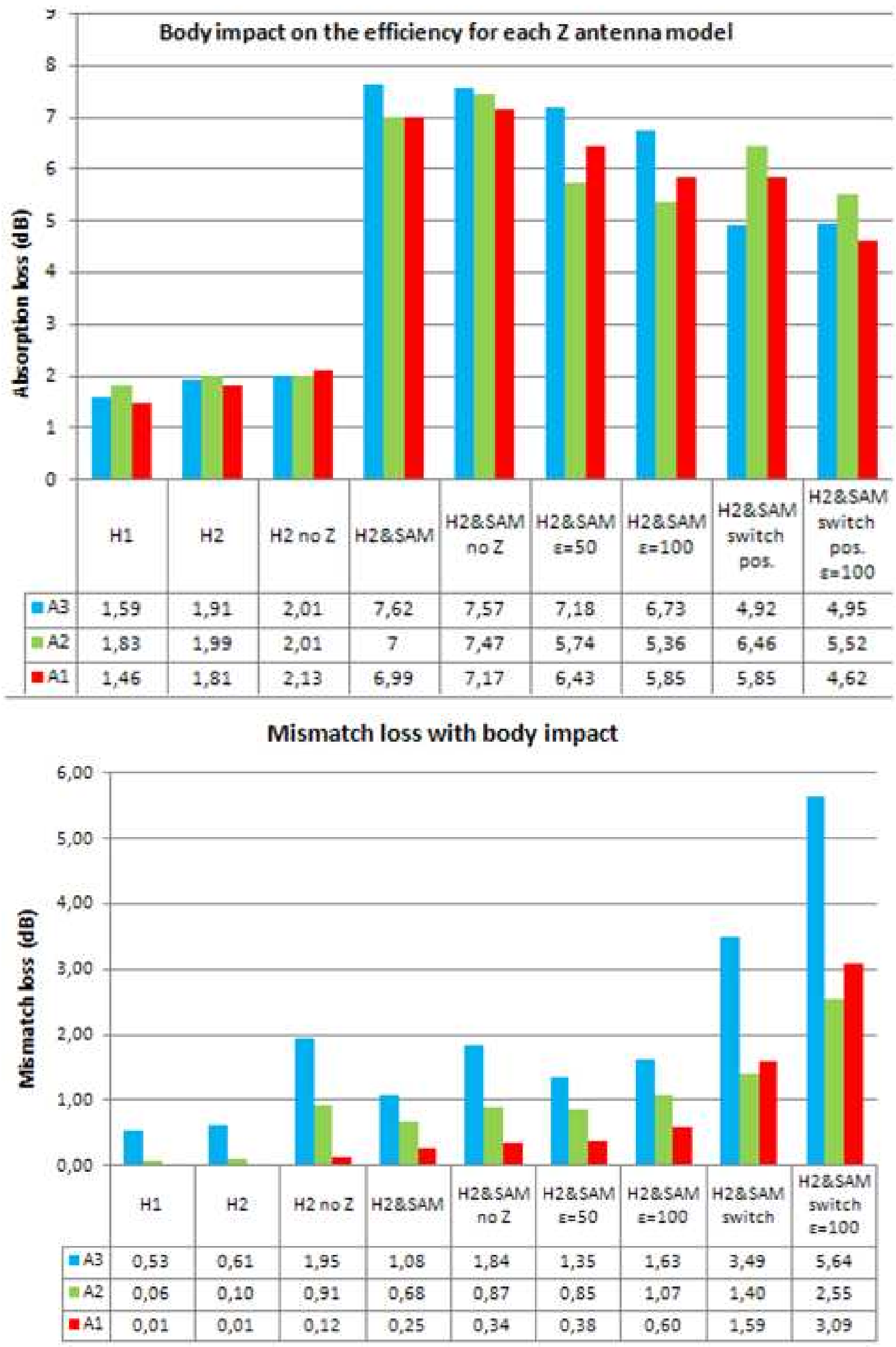

Figure 5.14: Absorption and mismatch loss in dB due to the proximity with the user's body. Influence of two hands phantom (H1 and H2) is compared. The influence of the head and a high permittivity layer between the Z antenna and the index finger as well.

Chapter 6

ANALYSIS AND EXPLANATIONS

6.1 Monopole and Z element

Recently, it was shown that adding a Z element to an antenna perpendicularly and in the middle of an infinite ground plane highly increases the matching to the source and that a additional matching circuit would not be needed anymore which enhances the efficiency of the resulting antenna. [16] This antenna structure was adapted to the small antennas application.

A successful configuration have been found which fits with the mobile phone requirements and keeps the position of the Z element with respect to the monopole. So the way how the monopole couples with the Z element is preserved. Then it can be hoped that the natural-matching property will be preserved. But the resulting antenna configuration implies that the Z element is not fed anymore.

The results for the Starting Design show that the matching is up to 45 dB (30 dB more than for the same monopole without the Z element) and the bandwidth is 2GHz. Then, the Z element still acts as a natural matching element and enhances the antenna properties.

The Z element still has its matching property even though it is not in contact with the source, the ground plane or the monopole. This is because it is close enough to the monopole (1mm) for that the radiated E and H fields from the monopole induce current flowing in it and permit the Z element to re-radiates secondary E and H fields, which will modify the resulting radiation pattern.

Another important condition to achieve very good matching to the source is that both the monopole and the Z element resonates in the exact same frequency. Then it is not enough to make longer the monopole in order to tune the resulting antenna structure to lower frequencies. To change the resonance frequency of the Z element all its parameters (length, width, etc.) should be changed. This tuning is quite tough and unpredictible.

It has been shown [16] that the Z element follows the formula : $f_r = \frac{1}{2\pi\sqrt{LC}}$.

In the starting design the Z structure can be modeled with coil and capacitor where : the coil has an inductance L = 0.86 nH and the capacitor a capacitance C = 1.95 pF. Since the inductance is greater than the capacitance, the coil will be changed in order to get lower resonance frequencies.

6.2 Coil and parallel capacitor

The Z element is placed at 1mm from the monopole, then in its very reactive near field. It is 2mm thick and a coil is place on top of it.

To tune the Z element, different kinds of coil have been tried with different inductances related to the sizes and the relative permeability of the materials. The exact value of inductance needed can be calculated theoretically with the previous formula but since the Z element is not connected to the source the theoretical and simulated resonance frequencies dont exactly match. But it is still usefull to have a range in which simulate the coil associated to the inductance values.

Because of the phone requirements, the coil couldn't be made too big and the lowest frequency that could be achieved was 2.6 GHz which correspônds to one band of the LTE. In this structure the coil was an 8 turns wire around a μ_r= 60 layer, which leads to an inductance L=1.6nH.

Also, because of the thickness of the Z element, the coil was 3mm far from the monopole. Then the E and H fields that where hitting it or re-radiated from it had smaller impact to each other. And the tuning was requiering higher inductances than theoretically.

Then a second structure has been designed where the Z element is cut in its middle and the coil inserted in between the two "J's" that form the "Z" shape. In this new case, the coil is 2 mm far from the monopole and composed by an 6 turns wire around a μ_r= 50 layer, whih leads to an inductance L=0.7nH. The resonance frequency of this second model is 2.45 GHz, the license-free band. Notice that the inductance is smaller in the second design and the resonance frequency is shifted lower, the opposite that what was expected. This is first because by cutting the Z element the capacitance changed ; and second because the coil being closer and still in the near field it is hit and re-radiating differently. The direct coupling between the monopole and the coil is stronger and added to the effect of the current flowing into it from the Z element.

The third structure is resonating in the same band : 2.45GHz but doesn't include a coil anymore. It includes a capacitor in parallel.

The primary coupling between the Z element and the monopole is equivalent to a capacitor and implies that the E field is contained in the x,y plane. In the two previous configrations, the coil was place in serial with the two "J's" to form a Z element. Then placing a capacitor in the y,z plane would be in parallel with the Z and from the microwave engineering we know that a parallel capacitor can act in similar way to a serial coil. These assumptions were verified by the simulations. The capacitor (3mm long, 6mm away from the monopole, 5nF) allowed a resonance frequency of the resulting antenna at 2.45 GHz and a matching up to -27 dB (20dB enhancement in comparison with the monopole alone).

6.3 User's influence

6.3.1 Absorption loss

For all the simulated cases, the results are summarized in the graphic of Fig. 5.0.6.4. In the 'soft' grip mode (H1) the losses are about 0.4 dB smaller than in the 'firm' grip mode, which places the index finger closer to the antenna area and the palm almost in contact with the ground plane. For the 'firm grip', the presence of the Z element and the SAM's head will be tested. The comparison with the simulations for the same monopole without additional Z element shows that the simple presence of Z reduces the absorption loss (AL) due to the hand of half-dB, depending on the models (the biggest reduction is for A1, then A3, then A2). Same results are found for the simulations with hand and head (A2 shows the biggest reduction, then A1, then A3). Also, the presence of a high permittivity layer between the index and the Z antenna (Z element side) is tested. It reduces the absorption loss for the hand and head case of 2.1 dB for A2. Finally a reverse configuration has been tried for the same models by switching the position of the monopole and the Z element. In other words, the monopole is no longer in the ear area but in the index finger one and the Z element is close to the ear. The best improvement is for A3: the AL goes from 7.62 dB to 4.92 dB by switching the monopole and Z element positions. And, from 6.99 dB to 4.62 dB for A1 by adding a high permittivity layer between the monopole and the index finger.

6.3.2 Mismatch loss

For all the simulated cases, the results are summarized in the graphic of Fig. 5.0.6.4. The mismatch loss (ML) is mostly due to the detuning of the Z antenna, overall when the monopole and the Z element are switched. A3 is the most deteriorated antenna by the presence of the user's body. A1 is the most resistant to the detuning. Again, the presence of the Z element in the antenna decreases the losses. For A3 and the 'firm' grip H2, there is 1.34 dB difference by just adding the Z element to the monopole. For the same antenna there is 0.8 dB difference in the simulation with hand and head. And, there is 0.55 dB difference by adding a high permittivity layer in between the Z element and the index finger.

Chapter 7

CONCLUSION

The electrically small Z antenna for mobile phone application, as presented in this report, is inspired from the Z antenna for UHF and VHF frequencies.

It has been adapted to the mobile phone requirements by translating it, rotating it and shrinking it. In this new structure the additional Z element is detached from the ground plane but still acts as a natural matching electromagnetical object.

The electrically small Z antenna for mobile phone application provides nearly complete natural matching to the source without the need of an external matching circuit. The simulations proved 30 dB enhancement for the $|s11|$ depth. This occurs when both Z element and monopole are properly matched with respect to each other. Then the overall efficiency is enhanced. Also, the gain patterns indicate that the Z antennas are more directive compared to the same monopoles, without Z element.

The tuning of this antenna doesn't need to revise its entire structure but only to change the lumped element on the top of it. In fact, by increasing the inductance from 0.86 nH to 2.16 nH, the resonance frequency could be lowered of 1.45 GHz.

The serial coil that determines the resonance frequency could be changed for a parallel capacitor. This change allowed to lower even more the resonance frequency of the resulting antenna and to keep the matching property.

The absorption and mismatch loss of the electrically small Z antenna for mobile phone application have been studied. The simulations included two hand grips, a 'soft' one and a 'firm' one and a head (SAM). The results showed that the presence of Z reduces the absorption loss due to the phantoms of 0.5 dB and the mismatch loss of 0.8 dB.

The presented antenna resonates at 2.45 GHz, the license-free band. To immediate talk mode application, the model should be improved lowering its resonance frequency to the GSM band. Because of the mobile phone requirements, the matching element (coil or capacitor) couldn't be tuned to reach the GSM. The 900 MHz - 1.8 GHz band could be achived by changing the antenna model, i.e. to an IFA or a PIFA. The capacitor narrowed the bandwidth to 50

MHz. This parameter could be improved with a model including both coil and capacitor in order to control the bandwidth.

Chapter 8

BIBLIOGRAPHIE

[1] A. Erentok and R.W.Ziolkowski, "Metamaterial-Inspired Efficient Electrically Small Antennas", *IEEE Transactions on antennas and propagation*, Vol. 56, No. 3, March 2008
[2] Z. N. Chen, "Antennas for portable devices", p14-16, 2007
[3] Gert F. Pedersen and J. B. Andersen. "Handset antennas for mobile communications: integration, diversity, and performance."
[4] V. G. Veselago, "The electrodynamics of substances with simultaneously negative values of ε and μ", *Sov. Phys. Usp*, Vol. 10, No. 4, 1968
[5] Constantine A. Balanis. Antenna theory, analysis and design. John Wiley & Sons, 3. edition, 2005.
[6] M. N. O. Sadiku, "Deficiencies in the way scattering parameters are taught", *IEEE Transactions on education*, Vol. 46, No. 3, August 2003
[7] David Pozar. Microwave Engineering.
[8] D. R. Smith, J. B. Pendry, M. C. K. Wilshire, "Metamaterials and Negative Refractive Index", *Science*, Vol. 305. No. 5685, pp. 788-792
[9] Y. Hao, R. Mittra, "FDTD modeling of metamaterials", 2009
[10] M. C. K. Wiltshire, "Metamaterials for Lenses and Cloaking from DC to Optics", *Antennas & Propagation Conference*, 2009
[11] R. Marques, F. Martin, M. Sorolla, "Metamaterials with negative parameters", 2007
[12] J. B. Pendry, A. J. Holden, D. J. Robbins and W. J. Stewart, "Magnetism from conductors and enhanced nonlinear phenomena", *IEEE*
[13] E. Ekmekci, G. Turhan-Sayan, "Comparative investigation of resonance characteristics and electrical size of the double-sided SRR, BC-SRR and conventional SRR type metamaterial for varying substrate parameters", *Progress In Electromagnetics Research B*, Vol. 12, 35-62, 2009
[14] Wu, B.-I., W. Wang, J. Pacheco, X. Chen, T. Grzegorczyk and J. A. Kong, "A Study of Using Metamaterials as Antenna Substrate to Enhance Gain", *Progress In Electromagnetics*, 2005
[15] H.H.Lin, C.Y.Wu, S.H.Yeh, "Metamaterial Enhanced High Gain Antenna for WiMAX Application", IEEE 2007

[16] R. W. Ziolkowski, "An efficient, electrically small antenna designed for VHF and UHF applications", *IEEE antennas and wireless propagation letters*, Vol. 7, 2008

[17] R.W. Ziolkowski and A. Erentok, "Metamaterial Based Efficient Electrically Small Antennas", *IEEE Transactions on antennas and propagation,* Vol. 54, pp.2113-2130, July 2006

[18] R.W. Ziolkowski, P. Jin, J. A. Nielsen, M.H. Tanielian and C. L. Holloway, "Experimental Verification of Z Antennas at UHF Frequencies", *IEEE antennas and wireless prpagation letters,* Vol. 8, 2009

[19] G. Poilasne, "Using EZ Antennas to Achieve Higher Design Efficiency", *Manufacturing Rayspan MTM antennas*, Rayspan Corp. 2010

[20] F. Capolino, "*Theory and Phenomena of Metamaterials*", 2009

[21] E. B. Rosa, "Self and Mutual Inductances of Linear Conductors", *Bulletin of the Bureau of standards*, Vol. 4, No. 2, p301-344
Transactions on microwave theory and techniques, Vol. 47, No. 11, November 1999

[22] M. Pelosi, O. Franek, M. B. Knudsen, M. Christensen and G. F. Pedersen, "A Grip Study for Talk and Data Modes in Mobile Phones", *IEEE Transactions on antennas and propagation*, Vol. 57, No. 4, April 2009

Appendix A

Simulations with a Z antenna

The design presented in Chapter 4 is inspired from the Z antenna but also fits with the handsets requirements. Let's first remember the Z antenna, as presented in the paper[16].

A.1 Z antenna structure

The Z antenna structure consists in a circular ground plane on which is placed, perpendicularly, a Z-shaped metallic sheet and a monopole, both connected to the source. It is shown in Fig. A.1

A.2 First designs

The first simulation was very close to this design. It is shown on the Fig. A.2

But this design cannot be efficient in mobile phone cases because : the antenna being in the middle, the repartition of the available space for the other components will be inapropriate and the battery cannot fit.

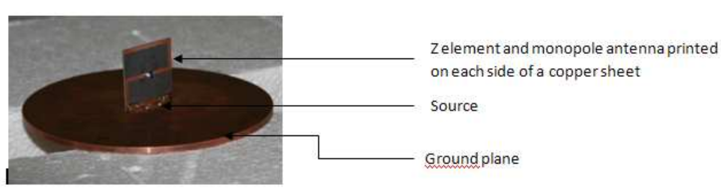

Figure A.1: The Z antenna [16]

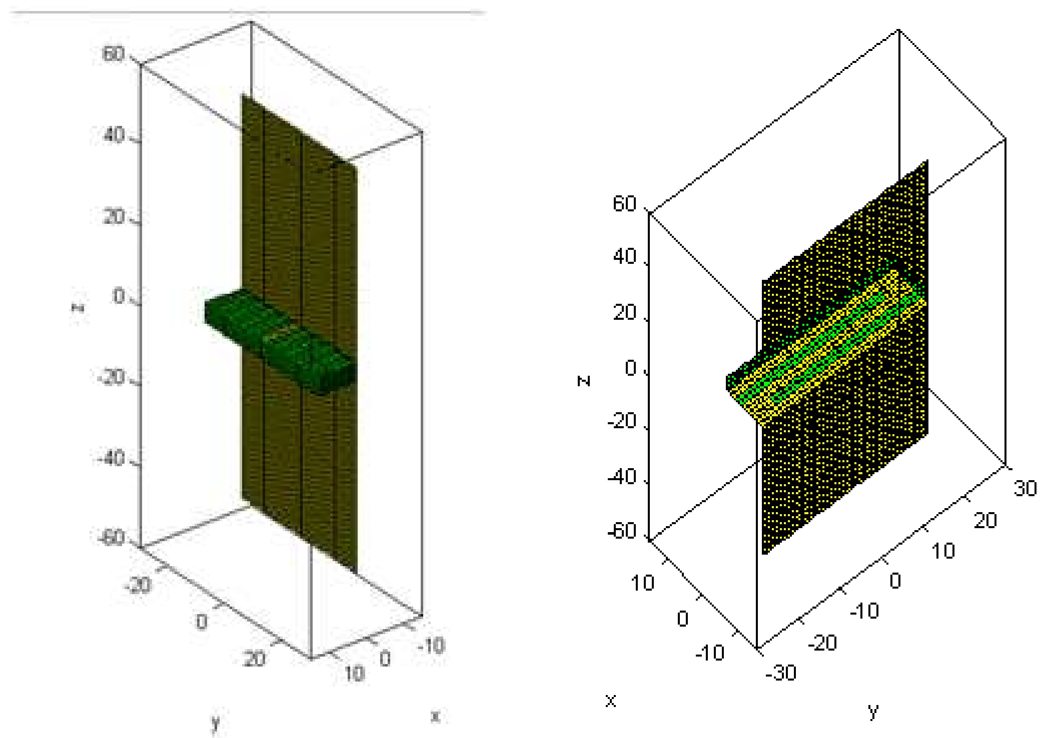

Figure A.2: First Simulation (a : monopole view, b : Z element view), reproduction of the Z antenna as presented in the paper[16]

A.3 Moving the structure in the top of the phone

Then, the whole antenna structure has been moved to the top of the phone, Fig. A.3

But the antenna cannot be longer than 10mm and then the resonance frequency is very high. Different permittivity and distances between the Z element and the antenna have been tried, but no one brought good results.

|s11|

To have the possibility to increase the length of the antenna, the monopole has been rotated in the y-plane instead of the x-plane. Then, a battery has been added in order to be closer to realistic models. In addition to that, the ground plane has been cut in the antenna area. The final figure is represented in Fig. A.4

All the length, from y=5mm to y=40mm, have been tried without any concluding result.

Also, the Z element and the antenna have been switched position as shown in Fig. A.5

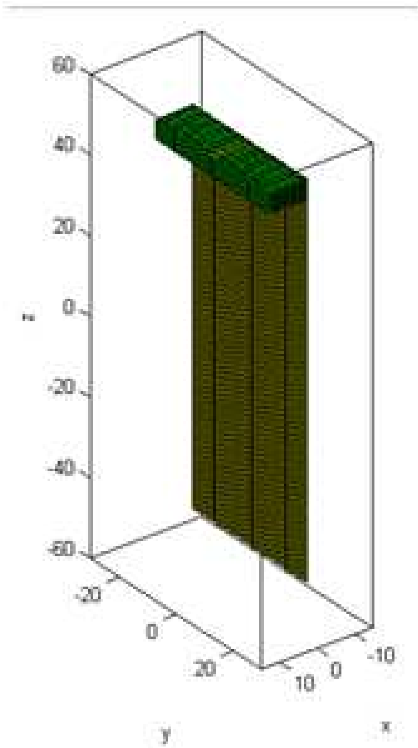

Figure A.3: Antenna structure on the top of the phone, monopole view

The following step was to rotate the antenna and design it parallel to the ground plane : Fig. A.6

Different positions of the Z element around the antenna have been tried. The dielectric block between the monopole and the Z element has been removed to see more easily the designs. The antenna has been folded to make it longer. The proposed designs are represented on Fig. A.7

A.4 Final design

Then the monopole has been folded to use more efficiently the space and make longer the monopole. And, the Z element has been rotated too in order to keep the coupling as originally designed. The final design came up with a very good matching. It is presented in Fig. A.8. Also is presented a comparison of the |s11| and the gain for the monopole itself and the monopole enhanced with the Z element.

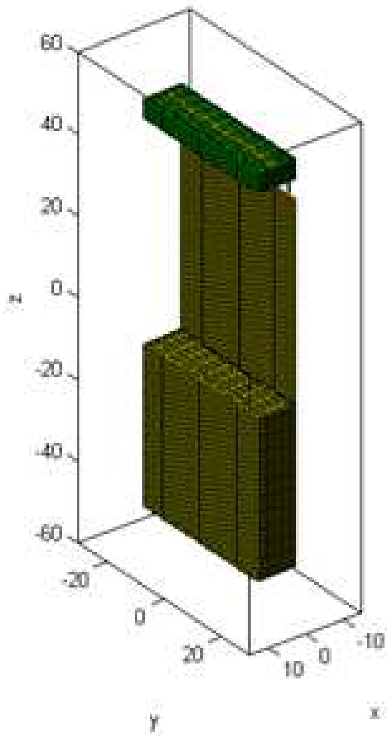

Figure A.4: Horizontal monopole in the Z antenna structure

A.5 CONCLUSION

In the 5 GHz design, adding the Z element improves the matching from -18dB to -36dB. Also it decreases the resonance frequency from 5.28GHz to 5.11GHz. The -6dB bandwidth is reduced when the parasitic element is added from 997MHz to 739MHz. The gain globally keep the same shape in all the planes and show improvements up to 2 dB : at 30° and 300° in G xy plane, at 90° in Gxz plane and between 30° and 150° in the Gyz plane. There is not any noticable reduction towards the head.

The properties of the Z element are still working even if the Z element is not connected to the ground plane.

But the resonance frequency is very high (about 5GHz) and is not appropriate to the mobile phones. Then the antenna and the Z element should be tuned. For this, a coil will be added to the Z element.

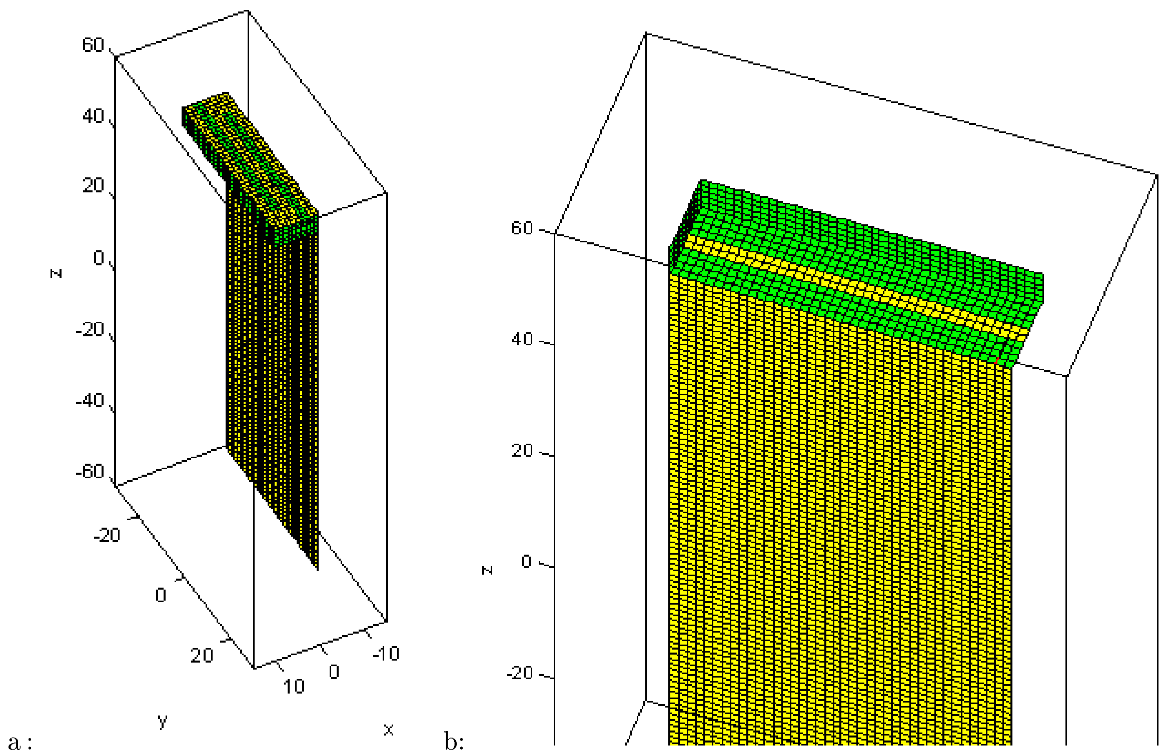

Figure A.5: Inverted position for the Z element and the monopole (a:Z element view, b:horizontal monopole view)

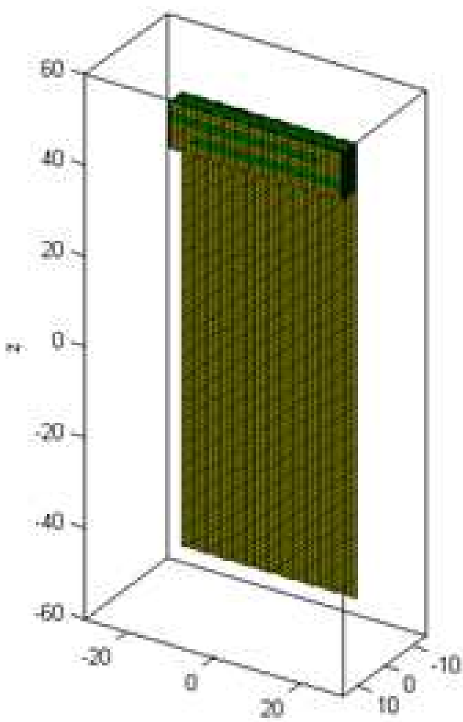

Figure A.6: The antenna structure parallel to the ground plane

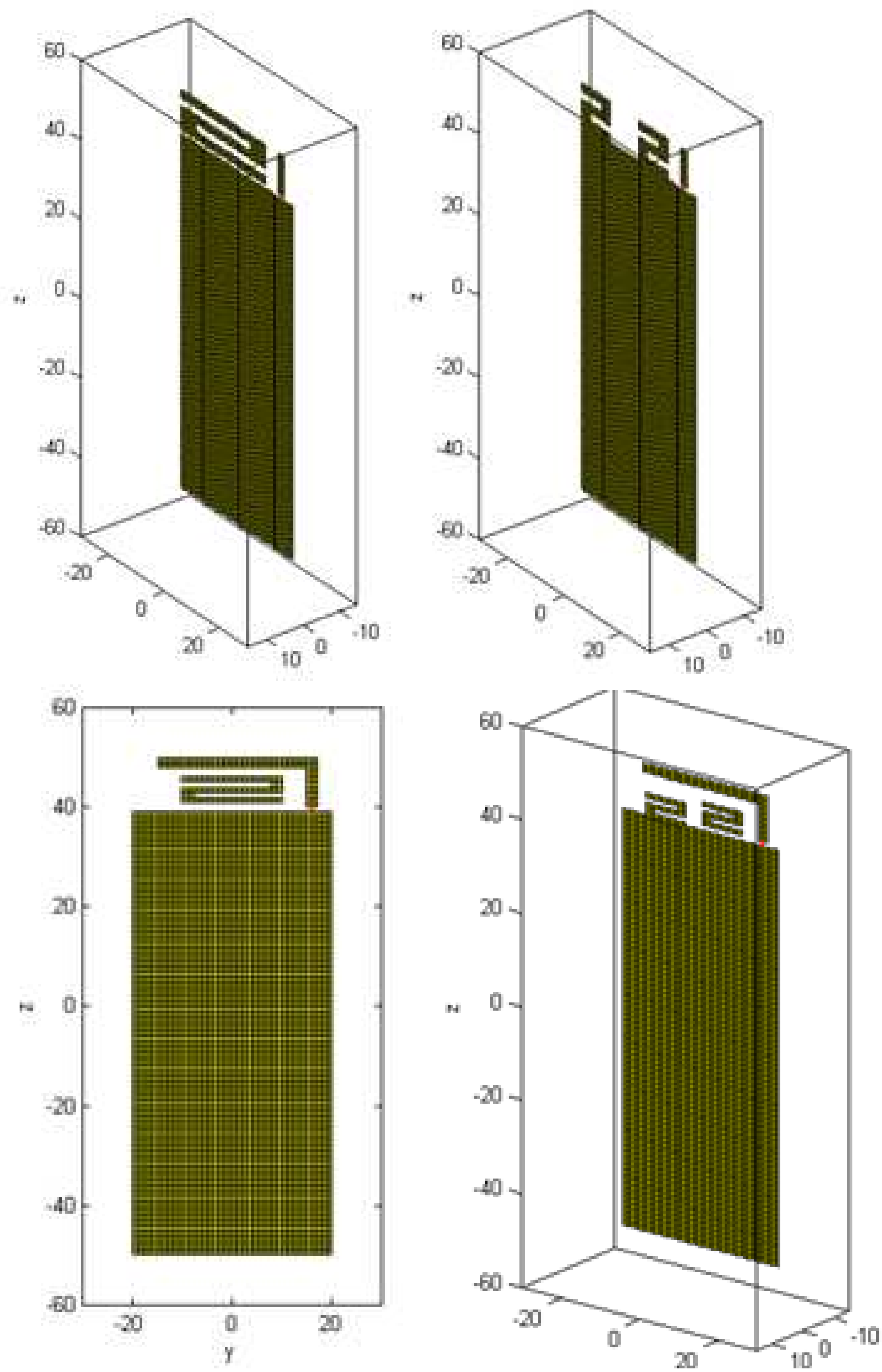

Figure A.7: Monopole parallel to the ground plane, no superposition between the Z element and the monopole

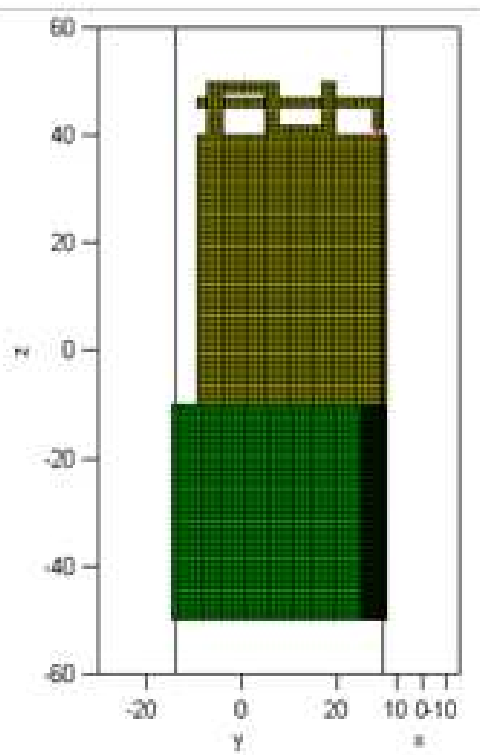

a:

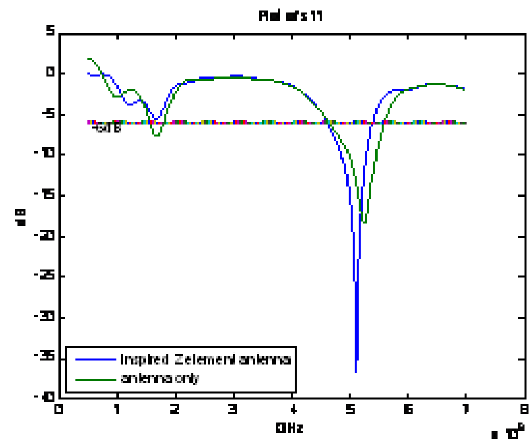

b:

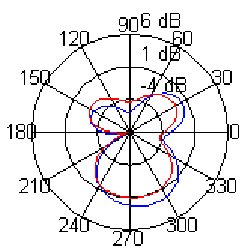

c:Gxy

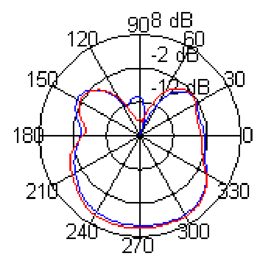

d:Gxz

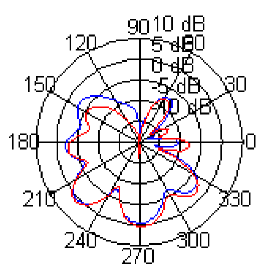

e:Gyz

Figure A.8: Final design (a:simulated antenna with phone requirements, b:|s11| parameter, c,d,e:in red the monopole only - in blue the Z antenna structure)

Appendix B

Tuning the Z antenna structure with a coil

In order to reduce the resonance frequency of the antenna, a coil as been placed on the Z element. It is shown [16] that the resonance frequency of the Z element respect this relationship :

$$f_r = \frac{1}{2\pi\sqrt{LC}} \tag{B.1}$$

Then by placing a coil on the Z and increasing its value, the resonance frequency should go lower.

The first way to model the coil was with a PEC 3D rectangle as shown in Fig. B.1

Different dimensions have been choose according with the space available. The coil dimensions are presented in the table below :

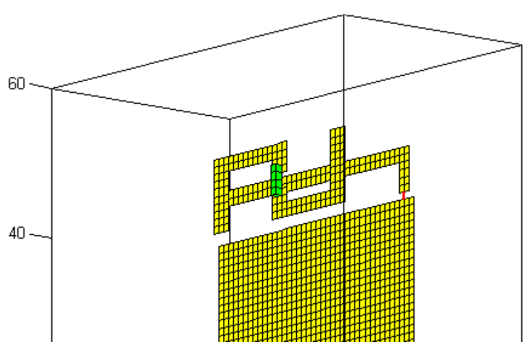

Figure B.1: layer coil has been added to the Z element

Dimensions (mm)	Inductance (nH)
1x1x1	0.22nH
2x1x1	0.78nH
3x1x1	1.44nH
4x2x2	1.56nH
4x1x1	2.17nH
6x1x1	3.76nH

The influence on the |s11| parameter is to decrease the resonance frequency while the value of the inductance increases. But the impact is very small. It is shown on Fig. B.2

Then to have biger values for the inductance, the coil has been represented by wire turns. The maximum number of turns is 10 in the space available, which represents a coil of inductance : L=4.8*10^{-7}H. The effect on the inductance is presented on Fig. B.3 with the comparison between the monopole alone, the monopole with the Z element and the monopole coupled with the Z element on the top of which there is a 10 turns wire coil.

it can be deduced that the monopole resonance is at 3 GHz, it gets higher when the Z element is added.

The Z element itself resonates around 2GHz. When a coil of inductance L=4.8*10^{-7}H is added, the Z element resonance is shifted form 2.5 GHz to 2.3 GHz. Therefore the wire coil (with larger inductance) has biger effect on the resonance.

Then, the length of the monopole has to be changed in order that both the monopole and the Z element with coil resonate at exaclty the same frequency. The right length of the monopole is now height h=9mm and length l=24mm. The resulting matching is as expected very good : |s11| goes until -50 db. This is presented in Fig. B.4

To go to even lower frequecies, the coil has to have a larger inductance but it cannot occupied more space, then a high permeability block will be added.

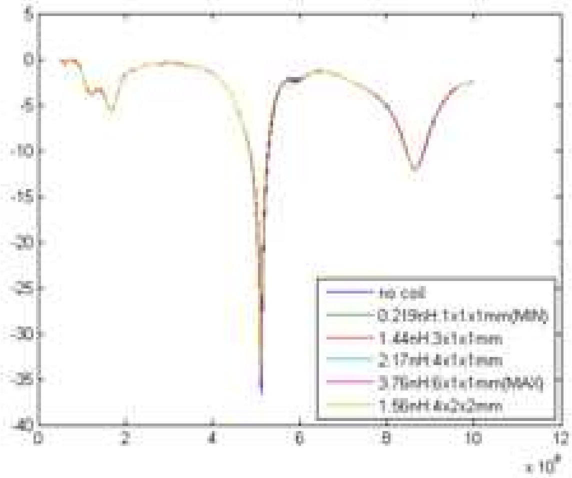

a:

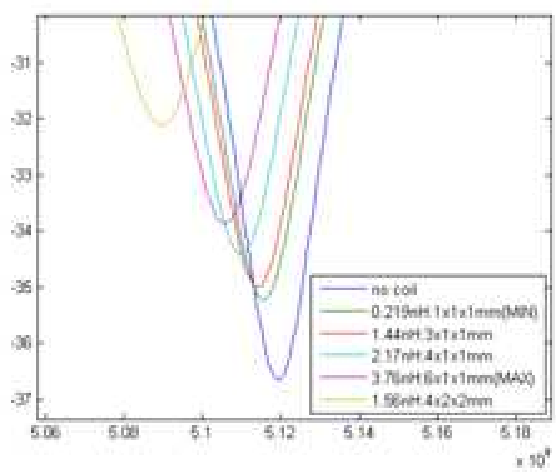

b:

Figure B.2: Influence on the resonance frequency of a 3D layer coil(a:normal view, b:zoom view)

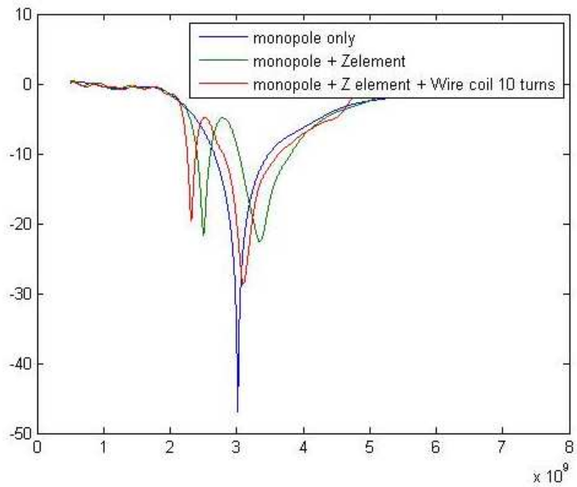

Figure B.3: Impact on a monopole of the Z element and the Z element with added coil

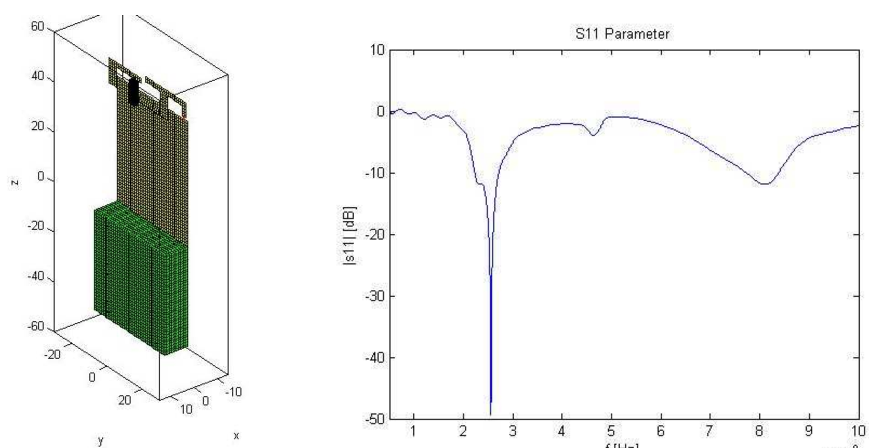

a: b:

Figure B.4: Antenna strucure tuned to 2.45 GHz with help of a coil L=4.8*10^{-7}H

Appendix C

FDTD : Yee cell

It is assumed that the medium is linear, isotropic and non-dispersive.

Yee algorithm is used to solve the E- and H- fields in time and space using the curl-equations. The Yee cell centers its E- and H- fields in 3D. The Yee algorithm centres its E- and H- fields in time.

So, according to Yee : the change in the E-field in time depends on the change in the H-field into space. In other words, at any point of the space, the updated value of the E-field in time is dependent on its stored value and also the local distribution of the H-field in space.

To achieve stability the following equation has to be respected :

$$\triangle t \leq \frac{1}{c\sqrt{\frac{1}{\triangle x^2} + \frac{1}{\triangle y^2} + \frac{1}{\triangle z^2}}}$$

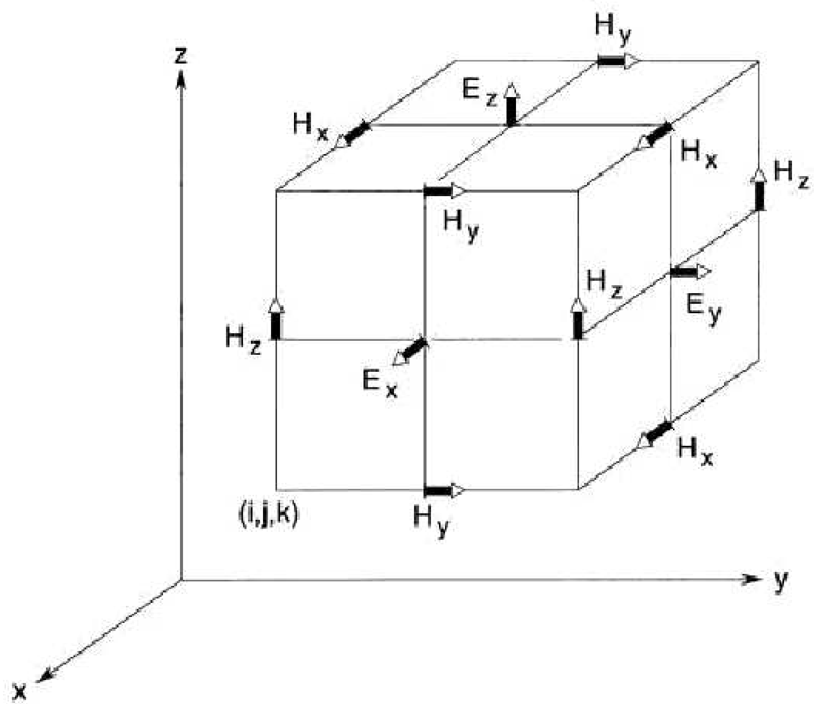

Figure C.1: Yee cell